Role of Pericytes in Hypertension-Related Cerebral Small Vessel Disease

by

Selin SAPANCI

A Dissertation Submitted to the

Graduate School of Health Sciences in Partial Fulfillment of the

Requirements for the Degree of

Doctor of Philosophy

in

Neuroscience

KOÇ ÜNİVERSİTESİ

August, 2024

Role of Pericytes in Hypertension-Related Cerebral Small Vessel Disease

Koç University

Graduate School of Sciences and Engineering

This is to certify that I have examined this copy of a doctoral dissertation by

Selin Sapancı

and have found that it is complete and satisfactory in all respects,
and that any and all revisions required by the final
examining committee have been made.

Committee Members:

Prof. Dr. Yasemin Gürsoy Özdemir (Advisor)

Prof. Dr. Mehmet Kaya

Prof. Dr. Ertuğrul Kılıç

Assoc. Prof. Dr. Vuslat Yılmaz

Assoc. Prof. Dr. Esra Özkan

Date: August 2024

Dedicated to my sweet daughter Doğa.

ABSTRACT

Investigation of the Role of Pericytes in Hypertension-Related Cerebral Small Vessel Disease

Selin Sapancı

Doctor of Philosophy in Neuroscience

August 2024

Introduction: The increase in the average life expectancy in society brings with it a decrease in cognitive capacity and the increase in the rate of dementia seen with aging as an important problem. The prevalence of occlusions in deep brain veins, small vessel disease, and white matter lesions grows as individuals age. Clinical research has demonstrated that these lesions significantly contribute to the decline in cognitive function. Hypertension (HT) is a chronic disease associated with small vessel disease, perivascular fibrosis and dementia. Perivascular fibrosis makes it difficult to clear waste materials from the brain. Recent studies suggest that pericytes may be responsible for this increased fibrosis.

Objective: In this study, we aimed to investigate the effects of pericytes on blood pressure values, disease course, cognition and brain fibrosis and waste material clearance by triggering HT in a transgenic pericyte ablation mouse model.

Method: To create conditional pericyte ablation, CreER+/- mice were crossed with Rosa26-DTA176+/+ mice. According to genotyping analysis, 28 animals that were CreER+Rosa26-DTA176+/+ positive were injected with tamoxifen for 2 days and their pericytes were ablated. 24 animals from the C57BL/6 breed were used as the control group. All animals were given angiotensin-II infusion of 1000ng/kg/day for 28 days by subcutaneous continuous infusion pump to create the HT model. Validation of the model was performed by measuring blood pressure from the tail cuff. In the last week of the

experiment, locomotor and cognitive changes were evaluated with open field, y-maze and novel object recognition tests. At the end of the experiment, all animals were injected with fluorescently labeled amyloid-beta (Aβ) via the cisterna magna. After 45 minutes, the clearance of Aβ from the brain in animals perfused was compared between the groups.

Findings: At the end of the one-month model, blood pressure values of the animals increased significantly compared to the initial measurements. Blood pressure measurements tended to be lower in the groups with pericyte ablated. In the open field test results, the total number of squares covered was significantly reduced in the pericyte ablation groups compared to the normal pericyte groups. When working memory and novel object discrimination index were examined in cognitive tests, they were lower in the pericyte ablation hypertension group. Clearance of Aβ from the brain was performed by scanning the marker in the intraventricular, pial arteries, intraparenchymal and pial veins. After 45 minutes, Aβ was observed only in the veins in the normal pericyte group, while in the pericyte ablation group, it was found that it spread widely to the parenchyma but did not reach the veins.

Conclusion: Pericyte ablation leads to lower blood pressure values in the hypertension model. It is also associated with significant locomotor slowness and delayed Aβ clearance and intraparenchymal accumulation. Therefore, healthy pericytes may be of critical importance in clearing toxic substances from the brain in the setting of HT and in protecting against dementia.

Keywords: hypertension, cerebral small vessel disease, blood-brain-barrier, pericyte, fibrosis

ÖZETÇE

Hipertansiyon ilişkili Serebral Küçük Damar Hastalığında Perisitlerin Patofizyolojideki Rollerinin Araştırılması

Selin Sapancı

Sinirbilim Doktora, Ağustos 2024

Giriş: Toplumda ortalama yaşam süresinin uzaması beraberinde yaşlanma ile görülen kognitif kapasitede azalma ve demans oranının artmasını önemli bir sorun olarak karşımıza çıkarmaktadır. Derin beyin damarlarında tıkanmalar, küçük damar hastalığı ve beyaz cevher lezyonları yaşlılıkla birlikte artmaktadır ve bu lezyonların kognitif kapasitenin azalmasında önemli rol oynadığı klinik çalışmalar tarafından gösterilmiştir. Hipertansiyon (HT), küçük damar hastalığı, perivasküler fibrozis ve demansla ilişkilendirilen kronik bir hastalıktır. Perivasküler fibrozis beyinde atık maddelerin temizlenmesini zorlaştırmaktadır. Son çalışmalar perisitlerin bu artmış fibrozisten sorumlu olabileceği yönündedir.

Amaç: Biz de bu çalışmada transgenik perisit ablate fare modelinde HT tetikleyerek, perisitlerin tansiyon değerleri, hastalık seyri, kognisyon ile beyinde fibrozis ve atık maddelerin temizlenmesi üzerindeki etkilerini incelemeyi amaçladık.

Yöntem: Kondisyonel perisit ablasyonu oluşturulması için, CreER+/- fareler ile Rosa26-DTA176+/+ fareler çaprazlandı. Genotipleme analizine göre CreER+Rosa26-DTA176+/+ pozitif olan 28 hayvana 2 gün tamoksifen enjeksiyonu yapılarak perisitleri ablate edildi. C57BL/6 ırkından 24 hayvan ise kontrol grubu olarak kullanıldı. Tüm hayvanlara HT modeli oluşturulmak üzere subkutan sürekli infüzyon pompası yerleştirilerek 28 gün 1000ng/kg/gün Anjiotensin-II infüzyonu verildi. Modelin validasyonu kuyruk manşonundan tansiyon ölçümü yapılarak gerçekleştirildi. Deneyin

son haftasında lokomotor ve kognitif değişiklikler açık alan, y-labirenti ve yeni nesne tanıma testleri ile değerlendirildi. Deneyin sonunda tüm hayvanlara sisterna magna yoluyla floresan işaretli amiloid-beta (Aβ) enjekte edildi. 45 dakika sonra perfüze edilen hayvanlarda Aβ'nın beyinden temizlenmesi gruplar arasında karşılaştırıldı.

Bulgular: Bir aylık modelin sonunda hayvanların tansiyon değerleri başlangıç ölçümlerine göre anlamlı olarak yükseldi. Perisit ablate olan gruplar tansiyon ölçümleri daha düşük olma eğilimindeydi. Açık alan testi sonuçlarında, perisit ablate olan gruplar da normal perisit gruplarına göre katedilen toplam kare sayısı anlamlı olarak azaldı. Kognitif testlerde çalışma belleğine ve yeni objeyi ayırt etme indexine bakıldığında perisit ablate hipertansiyon grubunda daha düşüktür. Aβ'nın beyinden temizlenmesi, intraventriküler, pial arterler, intra parankimal ve pial venlere belirtecin taranması ile gerçekleştirildi. 45 dakika sonra normal perisit grubunda Aβ yalnızca venlerde izlenirken, perisit ablate grupta ise yaygın olarak parankime yayıldığı ancak venlere ulaşmadığı tespit edildi.

Sonuç: Perisit ablasyonu hipertansiyon modelinde tansiyon değerlerinin daha düşük seyretmesine yol açmaktadır. Ayrıca belirgin lokomotor yavaşlık ve Aβ temizlenmesinin gecikmesi ve intraparankimal birikmesi ile ilişkilidir. Dolayısıyla sağlıklı perisitler HT zemininde toksik maddelerin beyinden temizlenmesinde ve demanstan korunmada kritik öneme sahip olabilir.

Anahtar Kelimeler: hipertansiyon, serebral küçük damar hastalığı, kan-beyin-bariyeri, perisit, fibrozis

ACKNOWLEDGMENTS

Foremost, my sincere appreciation goes to Prof. Dr. Yasemin Gürsoy Özdemir, whose unwavering support and unshakable belief in my capabilities have been instrumental. Your mentorship has not only dispelled my doubts but also emboldened me to explore new vistas. Collaborating with you has been an honor beyond measure.

My heartfelt gratitude extends to my esteemed committee members, whose insights and guidance have been invaluable assets throughout this academic pursuit.

A special thanks goes to Dr. Esra Özkan. Your faith in me has been a guiding light, showing that great dreams can indeed be achieved with unwavering perseverance. She's been like a true sister, guiding me and giving me advice. Even in the darkest moments, your laughter gave me courage. I am so lucky to have you by my side.

To my dear friends, Dr. Eda Kuşan Ünlü and Dr. Duygu Yazıcı you've made this whole doctorate journey better. I can't imagine what it would have been like without you. I will never forget the adventures we had during my PhD years, which helped to lighten up this challenging road.

I would also like to thank my dear friends at KUTTAM; Berkan Bozkurt and Sera Büşra Tekirdağlı. We have been through a lot, but we resist the struggle of life better together. I am sure you will always be successful. May the force be with you.

Together with the wonderful YGÖ team, we discovered a unique way to learn, work, and have fun together. We have always helped one another during this challenging journey. I would like to announce all your names, Fatmanur Akpunar, Feride Demirhan, Ali Burak Kızılırmak, Narges Shomalizadeh, Judy Kesibi, and Ceyda Özler.

My little Kemal Ege, who has made me happy with his existence since the first day he came into my life. What saved me from all this stress were those precious times we spent with you. You made my every day beautiful with your loving heart, beautiful games and your ways that always made me laugh. I'm so lucky that I was able to be your aunt! I will always be by your side in life, little man!

Finally, I am very grateful to my family. My family, my mother Zehra SELVİ, my father Oktay SELVİ, my sister Meltem MİRZA, and my brother Canberk MİRZA, have always been by my side throughout my life, without hesitating to make any sacrifices for my dreams. They have always contributed to my reaching this day, and have always ensured that I hold on to life strongly with their smiling faces.

I miss my uncle Tuncay SELVİ, who encouraged me to follow my heart and believe in the voice of my heart. I would also like to thank my aunt Selvihan DEMİRHAN, who has always supported me and made my life beautiful with her goodness, and my brother Hasan DEMİR.

I would like to thank my soul mate and superhero, Mehmet Furkan SAPANCI, who is always with me, who manages to make me smile even in my worst moments, and who makes my dreams eternal, for his existence.

Thank you with all my heart, I could not have made it through this journey without you!

I extend my heartfelt gratitude to all those who have played a pivotal role in shaping this journey and offering unwavering support as I traverse the realm of academia.

Funding

This project is funded by TUBITAK 1001 (121S608) grant and Koç University Research Center for Translational Medicine (KUTTAM).

TABLE OF CONTENTS

LIST OF FIGURES

ABBREVIATIONS

AD: Alzheimer's disease

AJ: Adherens Junctions

apoE: Apolipoprotein E

AT2: Angiotensin II

ATP: Adenosine triphosphate

Aβ: Amyloid-beta

BBB: Blood-brain barrier

BCSFB: Blood-Cerebrospinal Fluid Barrier

CADASIL: Cerebral Autosomal Dominant Arteriopathy With Subcortical İnfarction And Leukoencephalopathy

CMB: Cerebral microbleed

CNS: Central nervous system

CSF: Cerebrospinal fluid

CSVD: Cerebral Small Vessel Disease

DPBS: Dulbecco's phosphate-buffered saline

EEG: Electroencephalography

HT: Hypertension

i.p: Intraperitoneal

IFF: interstitial fluid

MRI: Magnetic Resonance İmaging

mRNA: Messenger ribonucleic acid

NG2: Neural/Glial Antigen 2

NO: Nitric Oxide

NOR: Novel object recognition

NVU: Neurovascular Unit

OFT: Open-field test

PDGFR-β: Platelet-Derived Growth Factor Receptor-B

PFA: Paraformaldehyde

RGS-5: Regulator Of G Protein Signaling-5

ROS: Reactive Oxygen Species

SC: Subcutaneous

STM: Short-term Memory

TJ: Tight Junctions

VaD: Vascular Dementia

WMH: White matter hyperintensity

ZO: Zonula Occludens

α-SMA: Alpha-Smooth Muscle Actin

µg: microgram

µL: microliter

µm: micrometer

µM: micromolar

%: percent

Chapter 1

INTRODUCTION

1.1. CNS Small Vessel Disease

Fisher originally reported the pathological characteristics of Cerebral Small Vessel Disease (CSVD) in 1960 (Fisher et al.,1982). Arterioles, capillaries, and venules are types of small blood vessels (Hakim et al., 2019). The histology definition of these small vessels is a vessel diameter of less than 1 mm, generally ranging from 50 to 400 μm (Cannistraro et al., 2019; Chojdak-Lukasiewicz et al., 2021). Classical locations for the cerebral small vessels include the paramedian branches of the basilar artery, the thalamus, the pons, the basal ganglia, and the subcortical white matter tracts, that contain the lenticulostriate branches of the anterior and middle cerebral arteries (Feekes et al., 2005). Cerebral small vessels form a unique interaction with adjacent cells in the brain parenchyma, functioning as a crucial component of the neurovascular unit. De Ciuceis et al. showed a negative correlation between CBF and tunica media/lumen diameter ratios in small resistance arteries utilizing brain tissue samples from hypertensive and normotensive individuals (De Ciuceis et al.,2014). The brain's vascular tree is unique from other organs since it is a part of the neurovascular unit (NVU), a term that was first used at the National Institute of Neurological Disorders and Stroke's 2001 Stroke Progress Review Group conference (Iadecola et al.,2017). The NVU consists of neurons, endothelial cells found within small blood vessels, vascular smooth muscle cells, pericytes, astrocytes, and other microglial cells (Figure 1.1) (Singh et al., 2023). The cells that constitute the neurovascular unit collaborate via a variety of intracellular and extracellular signaling pathways to create the blood-brain barrier, control cerebral blood flow in relation to neural activity, support fundamental neuronal processes, and remove metabolic waste products that might harm typical cellular processes. All vascular segments have a unique NVU architecture.

Although it is thought to play a role in both neurodegenerative and cerebrovascular diseases, the impact of architectural anomalies on function is poorly understood and a key area of neuroscience research interest (Iadecola et al.,2017).

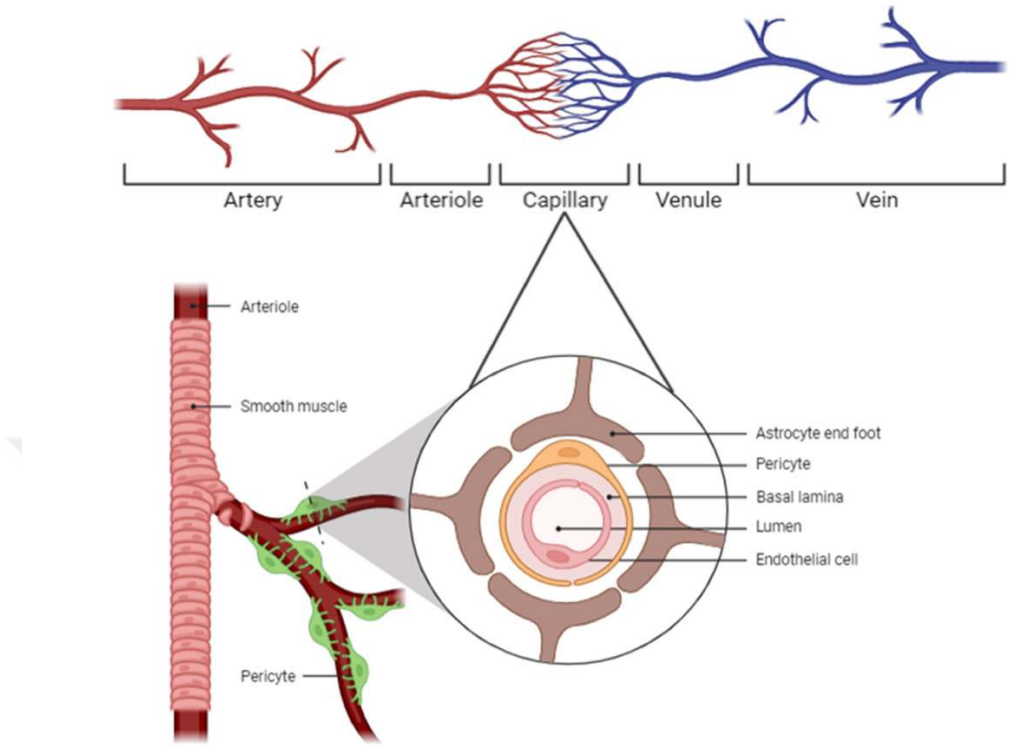

Figure 1.1 The neurovascular unit's constituent cells.

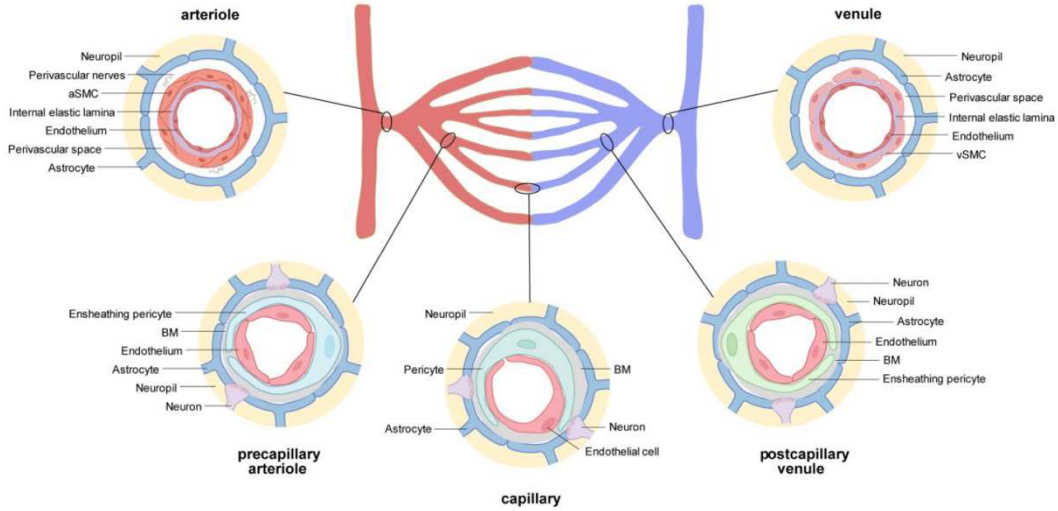

Figure 1.2 Overview of the cerebrovasculature (Wei et al., 2023).

CSVD is one of the most common pathological processes encountered by neurologists in clinical practice. The identification of CSVD was made possible by Fisher's postmortem pathological descriptions of lacunar palsy; however, the employing of MRI has led to a higher detection rate for CSVD. Lesions detected by magnetic resonance imaging (MRI) are considered as biomarkers of CSVD since small blood arteries in the brain are harder to observe directly than large ones. CSVD causes 45% of dementia cases and 25% of strokes. The prevalence increases with age, impacting nearly 100% of people over 90 years old to 5% of people over 50. CSVD can be asymptomatic; however, depending on the location, lesions can also cause symptoms such as mild cognitive dysfunction, dementia, mood disorders, motor and gait disorders, and urinary incontinence. Neuroimaging biomarkers such as including recent small subcortical infarctions, white matter hyperintensities, lacunes, cerebral microbleeds, enlarged perivascular spaces, and cerebral atrophy are used to diagnose CSVD (Fisher et al., 1982; Wardlaw et al., 2013) (Figure 1.3).

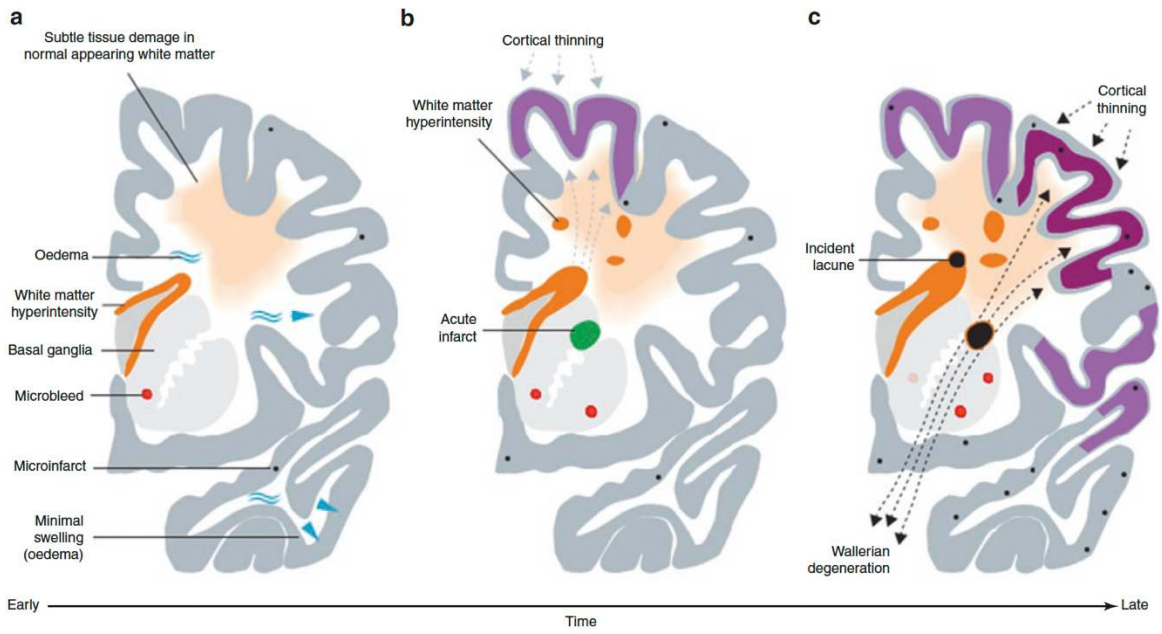

Figure 1.3 The brain as a whole is affected by small vessel disease.

The MRI progression of lesions associated with small vessel disease is shown from left to right. Be aware that incident lesions, such as infarcts and microbleeds, may not develop at all or may occur at different times as the disease progresses. Cortical thinning, brain atrophy, and neurodegeneration are the results of secondary loss of gray and white matter in connected brain regions and regions with less direct connections caused by acute

infarcts and white matter hyperintensities (observable on fluid-attenuated inversion recovery and T2-weighted MRI sequences). (a) White matter hyperintensity development results from minute alterations in normal white matter caused by increases in interstitial fluid. (b) Secondary cortical thinning results from the progression of white matter hyperintensities. Acute small subcortical infarcts might appear. (c) White matter hyperintensities, microbleeds, lacunes, secondary cortical thinning, and degeneration of the long tract worsen (Pantoni et al., 2010).

1.2. Epidemiology and risk factors

One of the main problems associated with society's increased average life expectancy is the aging-related decline in cognitive function and rise in dementia rates. Clinical research has indicated that white matter lesions, small artery disease, and occlusions in deep brain vessels all worsen with age and are major contributors to declining cognitive function (Figure 1.4) (Inoue et al., 2023). In terms of clinical prevalence, cerebral small vessel disease (CSVD) is the most frequent cerebrovascular disease. While the prevalence of CSVD increases with age; Differences such as gender, racial-ethnic, or geography have no known impact on prevalence (Cannistraro,et al., 2019 ; Hilal et al., 2017).

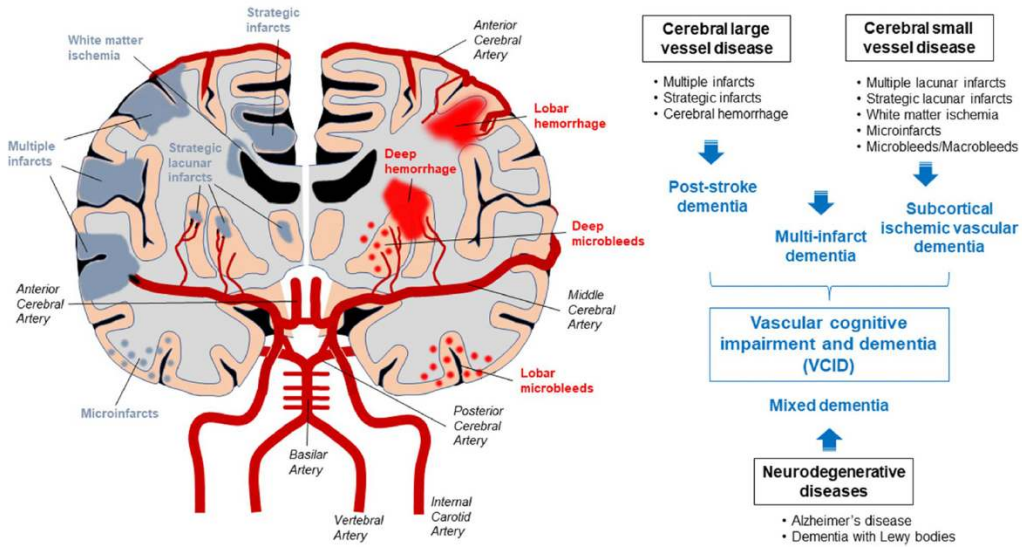

Figure 1.4 Cognitive impairment and dementia are caused by cerebral vascular lesions.

Specifically, as with White matter hyperintensity (WMH), the prevalence of Cerebral microbleed (CMB) increases in correlation with increasing age (De Leeuw et al.,2001; Poels, et al., 2010). The most significant modifiable risk factor for Cerebral Small Vessel Diseases is hypertension (Cannistraro,et al., 2019 et al). Other risk factors include diabetes, obstructive sleep apnea, current and former smoking, branch atheromatous disease linked to subcortical stroke, and chronic kidney disease (Khan et al., 2007; Kim, et al., 2013; Liu et al.,2018; Caplan et al., 2015). While single gene disorders are rarely the cause of CSVD, cerebral autosomal dominant arteriopathy with subcortical infarction and leukoencephalopathy (CADASIL) is probably the most common inherited cause of CSVD (Narayan et al., 2012). In cerebral small vascular disease, the true prevalence is substantially higher because most lesions are clinically "silent" and may not be "visible" on MRI. Therefore, it is crucial to treat the condition by taking into account all possible causes.

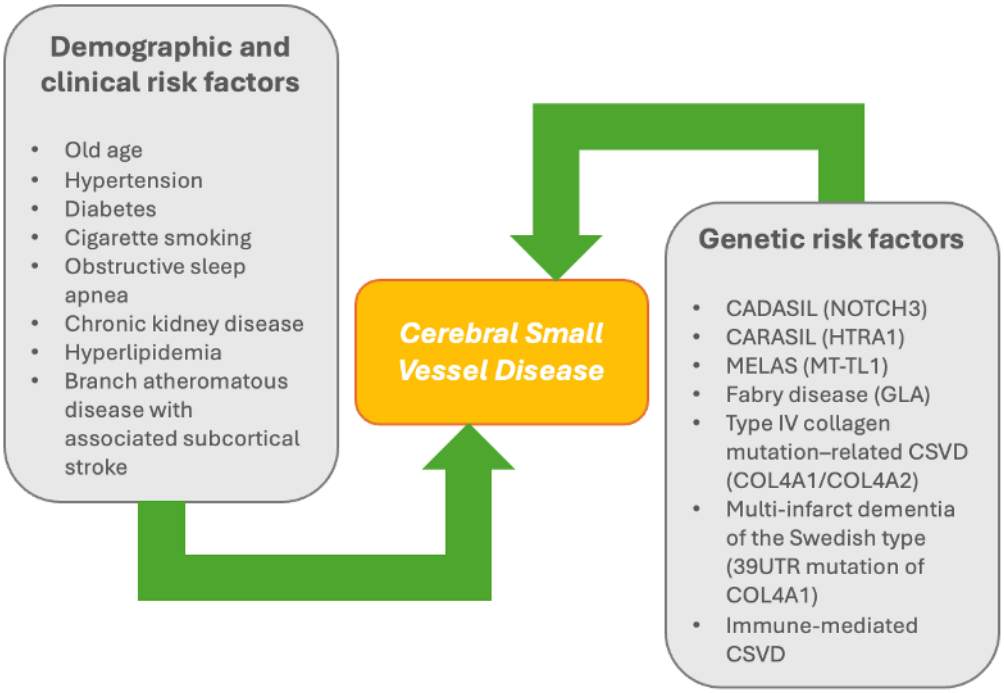

Figure 1.5 The risk factors of CSVD are summarized.

1.3. Hypertension

The rise in average life expectancy in society is accompanied by a decline in cognitive ability and an increase in the incidence of dementia, both of which are significant issues associated with aging. The prevalence of occlusions in deep brain veins, small vessel disease, and white matter lesions tends to rise with advancing age. Extensive clinical research has demonstrated that these lesions significantly contribute to the decline in cognitive function. Chronic hypertension is the primary risk factor for cerebrovascular dysfunction and stroke. Studies conducted on a population level have established a cause-and-effect association between hypertension and a decrease in cognitive functions. Furthermore, previous research has consistently demonstrated a robust correlation between brain imaging, namely brain MRI, and the extent of white matter lesions, as well as hypertension (Pasi et al., 2020). According to the American Heart Association, it is projected that half of the American population will develop hypertension by the year 2025. This rate is likely to be comparable or maybe greater in other nations, particularly in our own country, where hypertension is a significant issue. Hypertension causes damage to the blood vessels in the brain by various methods, including reducing the generation of nitric oxide (NO), increasing the creation of reactive oxygen species (ROS), and altering the structure of the extracellular matrix. There is a substantial correlation between hypertension patients and cerebral small vessel disease (CSVD), particularly in individuals over the age of 60. This association holds true regardless of whether the individual has hypertension or not. Lesions resembling small vascular disease have been identified in 80% of cases during MRI examinations, according to reports. Hence, alterations in the microvascular network of the brain, which impact the regulation of blood flow, may have a significant influence on the cognitive decline associated with hypertension (Gurol et al., 2020). Postmortem examinations have revealed that hypertension leads to the buildup of extracellular matrix elements, such as fibronectin and collagen, in the microcirculation of the brain. The medical term for this abnormal process is hypertrophic remodeling, which leads to the development of arteriosclerosis. Empirical evidence indicates that these alterations are linked to the accumulation of undetected lesions and cognitive decline, particularly in individuals with hypertension (Østergaard et al., 2016). The rising incidence of hypertension will result in a corresponding rise in the vascular consequences associated with these conditions. The serious economic

implications of this growth are unavoidable. The prevalence of dementia is experiencing a significant surge, with a projected threefold increase in the number of diagnosed patients worldwide by 2050, compared to the 46 million cases reported in 2016. Vascular dementia is the second most prevalent cause of dementia, following Alzheimer's disease (Prins et al., 2004). Moreover, the presence of hypertension-related cerebral small vessel disease significantly heightens the likelihood of developing both Alzheimer's disease and vascular dementia. Indeed, in research conducted on patients utilizing sophisticated imaging techniques, it was observed that 30% of those with Alzheimer's disease and 60% of those with other forms of dementia exhibited evidence of small blood vessel impairment. Autopsy studies, along with MRI and tomography imaging, have revealed a greater prevalence of occurrence (Launer et al., 2011; Prince et al., 2015). In addition, new studies have shown that the damage to the blood-brain barrier and vascular bed in Alzheimer's dementia directly affects the pathophysiological progression from the early stages (Nation et al., 2019). Although there is a wealth of clinical data and experimental investigations on Alzheimer's disease, there is a scarcity of controlled experimental models that utilize the latest technologies to study cerebral small vessel disease. The simultaneous occurrence of alterations in the vascular bed with hypertension (HT) and the cognitive decline process (early stage, medium stage, and late stage) is not yet understood. Understanding the mechanics of cerebral small vessel disease and the cognitive alterations caused by hypertension in this particular situation will have significant economic and societal benefits.

1.4. Blood-Brain Barrier

To maintain homeostasis, the central nervous system must efficiently transmit signals, tightly regulate the ion balance at synapses, and transport the necessary energy and materials from the circulation to the brain tissue. Due to this reason, the connection between brain tissue and the systemic circulatory system is distinct from that of other tissues. Consequently, the transportation of substances to the central nervous system is facilitated by the blood-brain barrier (BBB), which is a unique anatomical and physiological barrier (Gürsoy-Özdemir et al.,2017). The presence of such a barrier was first documented in Paul Ehrlich's research. The researcher injected water-soluble colors into the systemic circulation of animals and observed that all the dyes he examined

remained in peripheral organs, but were unable penetrate the brain tissue and spinal cord. The conclusions derived from these dye investigations led to the formulation of the notion of a partition between the blood and the brain, as well as between the blood and CSF (Serlin et al., 2015). The BBB is formed by the vascular endothelium, specialized basement membrane, pericytes, and astrocyte end-feet, starting at the cellular level.

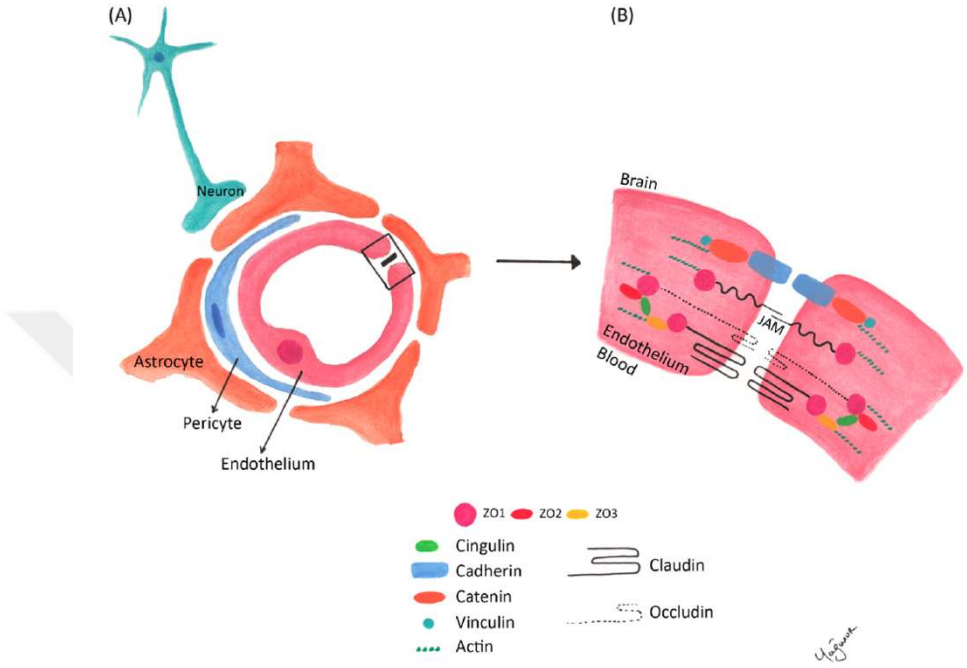

Figure 1.6 A) The BBB constituent cells. (B) Structure of tight (TJ) and adherens junctions (AJ) are schematized (Gürsoy-Özdemir et al.,2017).

The vascular endothelium plays a crucial role in regulating brain oxygenation, metabolite transport, and interstitial fluid balance by influencing cerebral blood flow, active and passive transporters, and fluid clearance (Iadecola et al., 2017). These processes primarily rely on the interactions between endothelial cells, pericytes, astrocytes, and oligodendroglial cells. Oligodendrocytes generate myelin, a substance that enhances the speed of signal transmission along axons. They are extensively connected and provide energy to maintain axons. Oligodendrocytes originate from oligodendrocyte precursor cells and are regenerated through the maturation of these precursors in the event of injury. Dysfunctional endothelial cells were found to hinder the development of oligodendrocyte precursor cells, leading to impaired myelination and myelin repair in a mouse model of sporadic small artery disease and in the histology of human white matter hyperintensities (Rajani.,2018). Cathepsin A-related arteriopathy with strokes and leukoencephalopathy

is a rare family small artery diseases. In this condition, there is also a disruption in the development of oligodendrocyte precursor cells due to endothelial dysfunction (Bugiani et al.,2016). Therefore, evidence from both sporadic and monogenic small vessel disease indicates that impaired endothelial cells can hinder the development and repair of myelin, as well as directly harm myelin through microvessel malfunction. Astrocytes establish connections between neurons and capillaries, with the astrocyte end-feet enveloping the outer surface of endothelial cells on one end and their processes coming into contact with dendrites on the other end. When neurons are active, astrocytes send signals to endothelial cells to enhance local blood flow and provide a sufficient supply of energy (Figure 1.7) (Iadecola et al., 2017; Rasmussen et al., 2018). Astrocyte end-feet possesses aquaporin-4, which are specific water channel proteins that typically orient towards the capillary. Aquaporin-4 molecules play a crucial role in controlling the movement of fluids through the interstitial space, which is necessary for maintaining the optimal environment for appropriate neuronal function. Aquaporin-4 molecules may translocate to the external surface of the astrocyte end-foot in regions of injury, as observed in human white matter hyperintensities (Rasmussen et al., 2018).

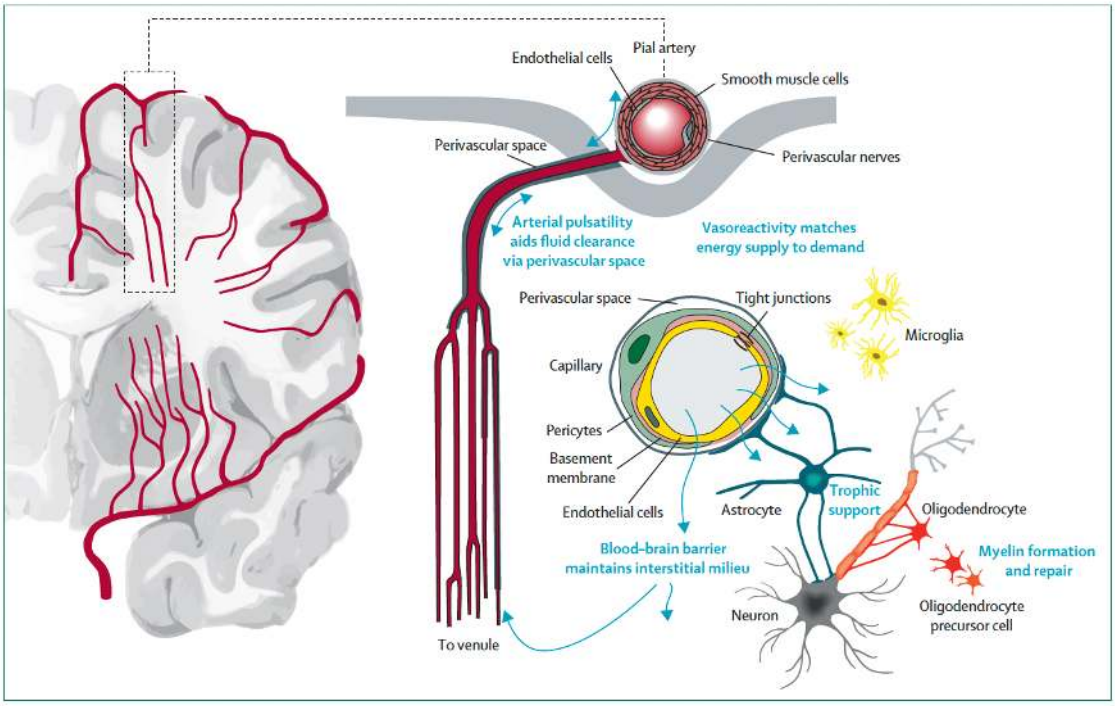

Figure 1.7 Key constituents of the vascular-glio-neuronal unit and possible entry points for disease mechanisms in cerebral small vessel disease (Wardlaw et al., 2019).

Dysfunction of the blood-brain barrier at the tissue level can have various negative effects. It can cause the leakage of fluids, proteins, and other plasma components into the surrounding tissues, leading to an increase in interstitial fluid (edema). This can also cause the thickening and stiffening of arteriole walls, which impairs the ability to further dilate blood vessels and transport oxygen and nutrients. Blood components can have detrimental effects through many mechanisms. For instance, after they pass through the blood-brain barrier, fibrinogen is broken down into fibrin, which triggers the activation of microglia and the recruitment of peripheral macrophages, leading to inflammation. Fibrinogen hinders the process of oligodendrocyte precursor cell development, which in turn inhibits the maintenance and repair of myelin. Additionally, it tightly attaches to amyloid-β, impeding its removal and encouraging the development of amyloid-β plaques and the loss of pericytes. Patients with Alzheimer's disease exhibit elevated levels of perivascular fibrin deposits, which may serve as a possible mechanism connecting small vessel illness and the development of Alzheimer's disease pathology (Petersen et al.,2018). The blood-brain barrier can experience subtle malfunction as a result of normal aging, but this process may be expedited by genetic predisposition. Genes like Foxf2, which are active in brain vascular endothelial cells and pericytes, have been associated with spontaneous small vessel strokes and white matter hyperintensities (Malik et al., 2018). The Notch3XR169C transgenic mice serve as a model for cerebral autosomal dominant arteriopathy with subcortical infarcts and leukoencephalopathy (CADASIL), which is the most common form of familial small vessel disease. These mice exhibit alterations in important components of the blood-brain barrier, including pericytes, astrocytic end-feet, and the extracellular matrix (Ghosh et al.,2015). Patients with vascular dementia and Alzheimer's disease experience more severe blood-brain barrier disruption (Nation et al., 2019). Multiple clinical studies have demonstrated the presence of blood-brain barrier failure in patients with stroke, cognitive problems, or small artery disease, as evidenced by abnormalities in biochemical (CSF or blood), neuroimaging, or neuropathology techniques (Li et al., 2018; Huisa et al., 2015; Zhang et al.; 2019; Wardlaw et al., 2017). The malfunctioning of the blood-brain barrier escalates as the burden of white matter hyperintensity increases (Zhang et al., 2019; Rost et al., 2018). There is evidence of the blood-brain barrier leaking in the normal seeming white matter of individuals with small vessel disease. This leakage becomes more severe as it gets closer to the white matter hyperintensity, which is a common location for future extensions of white matter

hyperintensity and the occurrence of lacunes (Duering et al., 2013; Huisa et al., 2015). According to one MRI study, the malfunction of the blood-brain barrier was more severe in the perilesional normal looking white matter compared to white matter hyperintensity. However, it is worth noting that other investigations have reported the opposite findings (Huisa et al., 2015; Wardlaw et al., 2017). Some neuropathology studies did not detect any disruption in the blood-brain barrier, which could be attributed to the intermittent or localized character of the problems or the challenge of identifying small alterations (Hainsworth et al., 2015). Corresponding to the dysfunction of the blood-brain barrier, the amount of fluid between brain cells increases in areas of white matter hyperintensities and in normal appearing white matter as the burden of white matter hyperintensities increases. The highest amount of fluid is found in white matter hyperintensities, followed by the surrounding normal appearing white matter, and then the more distant tissue. Additional indirect evidence supporting the idea that dysfunction in the blood-brain barrier plays a causative role in small vessel disease can be found in studies involving patients with acute lacunar stroke symptoms, or CADASIL (Wardlaw et al., 2017; De Guio et al., 2015). In these studies, it was observed that interstitial fluid and brain volume were higher when patients presented with stroke symptoms compared to several months later. This increase in fluid and volume was accompanied by a decrease in white matter hyperintensity, indicating that the reduction in hyperintensity and brain volume was not due to cell loss but rather the removal of excess interstitial fluid (Wardlaw et al., 2017). Three investigations discovered a correlation between blood-brain barrier disturbance during the initial evaluation and long-term consequences (Huisa et al., 2015; Wardlaw et al., 2013). An instance of blood-brain barrier failure in normal looking white matter was found to be a predictor of unfavorable functional outcomes. After a period of 3 years, it was observed that the dysfunction of the blood-brain barrier in the normal appearing white matter was able to predict cognitive decline 1 year after a lacunar stroke. Additionally, certain regions of the normal appearing white matter that had abnormal blood-brain barrier permeability at the beginning showed the development of new white matter hyperintensities on follow-up scans 1 year later (Huisa et al., 2015; Wardlaw et al., 2013; Wardlaw et al., 2017).

Subsequent research has shown that, apart from the blood-brain barrier (BBB), the central nervous system (CNS) possesses additional barriers. Additionally, three barrier layers contribute to the separation of blood and brain tissues. These layers are:

1. The BBB.
2. The blood-cerebrospinal fluid barrier (BCSFB) is formed by the choroid plexus epithelium, which releases specialized cerebrospinal fluid (CSF) into the cerebral ventricles.
3. The arachnoid epithelium acts as a barrier between the blood and the subarachnoid cerebrospinal fluid (CSF).

Nevertheless, these final two obstacles have a very small surface area in comparison to the actual blood-brain barrier and are not subject to stringent regulation (Gürsoy Özdemir et al., 2017; Abbott et al., 2006). Focusing on the blood-brain barrier, which is the main target of drug delivery to brain tissue, will increase the chance of treatment for neurodegenerative diseases.

1.5. What is a pericyte?

The brain, in terms of its mass, is the organ that demands the highest volume of energy in the body, and its needs for energy change fast. The neurovascular unit is a specialized structure that has evolved to fulfill the specific requirements of the brain. This unit is a complex structure composed of endothelial cells, astrocytes, neurons, microglia, vascular smooth muscle cells, and pericytes. It is situated between the brain parenchyma and capillaries. Pericytes are cellular structures that are found in the precapillary arterioles, capillaries, and venules in many parts of the body, with a higher concentration in the retina and brain. Pericytes have a role in the pathophysiology of several diseases due to their specific location and functions. Pericytes are dysfunctional in several disorders, such as dementia, stroke, diabetic retinopathy, and tumor angiogenesis. Pericytes, similar to vascular smooth muscle cells, show the expression of contractile proteins such as alpha-smooth muscle actin (α-SMA), myosin, and tropomyosin, enabling them to undergo contraction. Pericytes that are in closer proximity to the arterioles have increased α-SMA expression and have extensions that firmly circularly encircle the vessel. Pericytes located in the middle segments of capillaries show a lower degree of α-SMA expression. Their extensions are oriented longitudinally, allowing them to cover a larger area of the blood channel. However, they do not tightly encircle the vessel. Pericytes close to the tip of the venule also show a limited degree of α-SMA expression, and their extensions have a reticulated morphology. Although there is variation, central nervous system (CNS)

pericytes can be recognized and characterized by shared markers, including platelet-derived growth factor receptor-β (PDGFR-β), neural/glial antigen 2 (NG2), and regulator of G protein signaling-5 (RGS-5). However, the markers employed to identify pericytes lack specificity and can be expressed by different cell types, posing a challenge to accurately identifying pericytes. Pericytes in the neurological system perform multiple functions, such as regulating blood flow, developing and maintaining the Blood-Brain Barrier (BBB), promoting the growth of new blood vessels, controlling inflammation, and providing a source of stem cells.

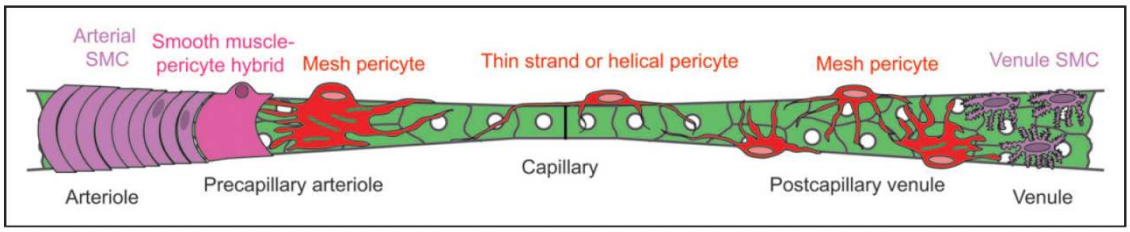

Figure 1.8 The pericyte forms are schematized (Hartmann et al., 2015).

The brain vessels, which are approximately 600 kilometers long, are composed of capillaries that make up 85% of their structure. The capillaries contain the endothelial cells of the blood-brain barrier, which are reinforced by tight junctions to minimize both paracellular and transcellular transmission. The capillaries are encircled by a distinct basement membrane, and pericytes located within the same basement membrane play a role in establishing the BBB during embryonic development and maintaining it in maturity. Pericytes play a crucial role in the formation and upkeep of tight junctions in the blood-brain barrier (BBB) and have an impact on the movement of substances across the endothelial cells. The blood-brain barrier (BBB) is mostly composed of claudin-1, -3, -5, and -12 proteins, as well as occludin. The tight junctions of the BBB are linked to the intracellular skeleton by zonula occludens (ZO)-1, -2, and -3. Studies have demonstrated that the loss of pericytes leads to the loss of claudin-5, occludin, and ZO1, or alterations in their arrangement. Moreover, besides impacting the tight junctions of pericytes, it has also been demonstrated to enhance the permeability of the blood-brain barrier by regulating the transit of substances through endothelial cells.

1.6. The Glymphatic System

The glymphatic system is a system for eliminating waste that employs a unique perivascular duct system formed by astrocytes to facilitate the effective removal of soluble proteins and metabolites from the central nervous system. The glymphatic system plays a critical role in the exchange of cerebrospinal fluid (CSF) around the brain and interstitial fluid (IFF) within the brain tissue by connecting the perivascular spaces (PVS) throughout the brain.The movement of CSF into the gaps around the arteries (known as glymphatic inflow) is essential for the brain's energy metabolism (Lundgaard et al., 2015) and signaling molecules (Rangroo Thrane et al., 2013). This process facilitates the transport of glucose, lipids and apolipoprotein E (apoE) generated from the choroid plexus (Achariyar et al., 2016). Furthermore, the glymphatic system's drainage of ISF is crucial for eliminating several metabolic waste substances, including amyloid-beta protein (Aβ) and tau, along with other solutes (Iliff et al., 2013). The mechanisms driving glymphatic flow have only recently begun to be elucidated.

Research focused on identifying the primary mechanisms that control the glymphatic system has uncovered multiple processes that are disturbed in diseased circumstances. These findings have improved our comprehension of the fundamental mechanisms of glymphatic dysfunction and have aided in the identification of events linked to different disease mechanisms. Research on glymphatic insufficiency in SVD emphasizes the significance of perivascular spaces (PVSs), brain pulsation, and clearance in the central nervous system (Mestre et al., 2017). It is suggested that various factors, including changes in blood vessel structure, the buildup of Aβ around blood vessels and in enlarged perivascular spaces (EPVS) and cerebral amyloid angiopathy (CAA), as well as the presence of granular osmiophilic material (GOM) in CADASIL, may impact the overall movement of fluid inside perivascular spaces (PVSs). Empirical evidence and quantitative modeling have demonstrated that PVS obstacles, such as protein clumps, have an impact on these flows (Asgari et al., 2016). The alterations in blood vessel wall compliance and reactivity, which are typical of SVD, are highly likely to have a considerable impact on these blood flows. Age-related and neurodegenerative illness models have demonstrated a considerable decrease in the clearance of toxic solutes such as Aβ in the central nervous system. This is especially pertinent for certain forms of SVD

distinguished by protein aggregation and buildup. Disturbances in the functioning of the glymphatic system have been associated with various processes related to aging (Kress et al., 2014), microinfarcts (Wang et al., 2017), stroke(Gaberel et al., 2014), Alzheimer's disease (Peng et al., 2016), migraine (Schain et al., 2017), and diabetes (Jiang et al., 2016).

Protein aggregation is a major characteristic observed in numerous neurodegenerative disorders. In the context of Alzheimer's disease, the aggregates known as Aβ and tau, in Parkinson's disease, the aggregate α-synuclein, and in Huntington's disease, the aggregate huntingtin serve as illustrative instances. This condition is also noticed in SVD types 2 and 3, where these accumulations usually appear on the outer surface of PVS. Recent investigations have shown that protein clustering inside the PVS has a negative effect on the function of the glymphatic system (Gaberel et al., 2014). This dysfunction has been found to have a role in the development of SVD. The presence of plasma-derived proteins, including fibrin/fibrinogen and albumin, is a characteristic hallmark of many forms of SVD and can also impact the flow of glymphatic fluid (Gaberel et al., 2014).

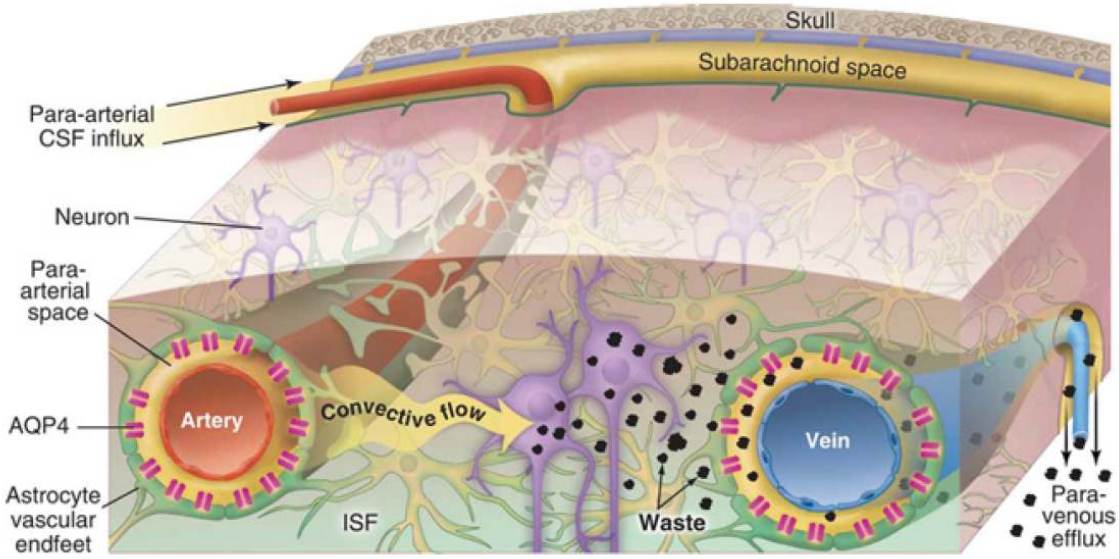

Figure 1.9 Overview of the glymphatic system (Mestre et al., 2017).

Chapter 2

MATERIALS AND METHODS

2.1. Pericytes Ablation with The Use of Transgenic Animals

We employed the CreER-LoxP system to establish our inducible pericyte ablation model. The loxP floxed sequences are excised from the genome using the tamoxifen-activated Cre Recombinase-Estrogen receptor fusion protein (CreER) in this method. Specifically, mice from two distinct genetic lines, namely PDGFRβ-P2A-CreER+/- (JAX Mice, 030201) and Rosa26-DTA176+/+ (JAX Mice, 010527), were bred together to achieve pericyte ablation that is reliant on both time and cell type. PDGFRβ-P2A-CreER transgenic mice possess a CreER gene that is regulated by the Pdgfrβ promoter, resulting in the production of CreER. The breeding partner of these mice, Rosa26-DTA176, carries a gene called diphtheria toxin (DTA176) that is expressed by a constitutive ROSA promoter. The Rosa26-DTA176 mice possess a loxP floxed stop gene located upstream of the DTA176 gene. Despite being present in all cells of the animals, the DTA176 protein cannot be effectively produced due to the presence of a stop codon preceding its mRNA sequence. Nevertheless, if there is Cre Recombinase activity in the cells, the stop codon will be removed from the DNA. Thus, only the cells that have the ability to produce the CreER enzyme, specifically the Pdgfrβ-positive cells in our experiment, will be able to generate a fully functioning diphtheria toxin protein. Consequently, Pdgfrβ-positive cells, which include pericytes, would be eliminated because of the particular expression of DTA in these cells after tamoxifen injection.

2.2. Genotyping

We generated a transgenic line for pericyte ablation by breeding DGFRβ-P2A-CreER (030201, Jackson Laboratory) mice with Rosa26-DTA176 (010527, Jackson Laboratory) mice. The Rosa26-DTA176 variant exhibits a uniform expression of the attenuated diphtheria toxin, DTA176. Thus, genotyping is required. Nevertheless, the expression of the CreER complex in the PDGFRβ-P2A-CreER line is varied. Therefore, in theory, only 50% of the offspring exhibit CreER based on Mendelian principles. A tail polymerase chain reaction (PCR) was used to identify CreER-positive offspring. In the beginning, DNA extraction from the tails was carried out using the Zymo Quick DNA Miniprep kit (Catalog Number D4069). Subsequently, polymerase chain reaction (PCR) was performed using the genomic DNA to amplify the Cre gene as the target product and the Pdgfrβ gene as an internal positive control (Figure 2.2). In order to visually represent the genotyping results, the PCR products were subjected to electrophoresis on a 1.5% agarose gel (Figure 2.1).

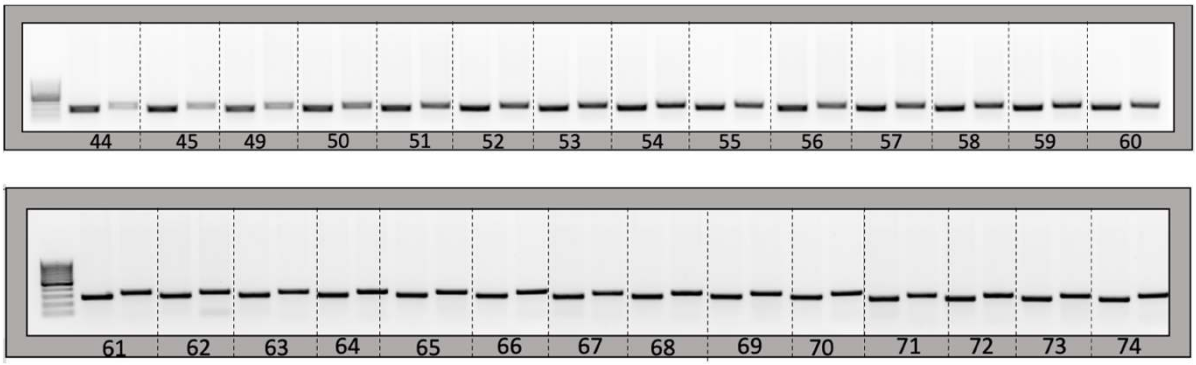

Figure 2.1 An example image of DNA electrophoresis results of genotyping

The numbers correspond to the unique identification codes assigned to the animals. Every animal possesses two polymerase chain reaction (PCR) products. The first one is generated by the internal control primers, leading to the duplication of the Pdgfrβ gene. The second lane consists of primers specifically intended to duplicate the Cre recombinase gene, but only if it is present. The first lane serves as the internal positive control to verify technical reliability, while the second lane indicates the presence of the Cre recombinase gene.

PDGFRβ-Cre/ Forward	CCA CCT TGA ATG AAG TCA ACA C
PDGFRβ-Cre/ WT Reverse	AGC TTG TGG CAG TGT AGC TG
PDGFRβ-Cre/ Mutant Reverse	ACA TGT CCA TCA GGT TCT TGC

Figure 2.2 List of Primers used in Genotyping

2.3. Hypertension Control and Pericyte Ablate Mice Model Creation

Angiotensin II (AT2) is continuously infused for four weeks, and an osmotic pump a recognized and widely used model in the literature—is employed to simulate hypertension in my experiment. Since the angiotensin pathway is the same mechanism that causes essential hypertension in people, the AT2 infusion model is considered a suitable model of primary hypertension in humans. In this regard, it is an excellent model to study the molecular mechanisms associated with RAA. Applications with varying dosages and durations have been employed in the past. We selected a high-dose application (1000ng/kg/min) for 4 weeks (chronic). This is due to reports that this dosage alters brain chemistry, damages the blood-brain barrier, and induces an organ's hypertrophic response and vascular remolding (Lerman et al., 2019). Transgenic mice with conditional pericyte ablation at adulthood (week 10) and control mice expressing normal pericytes were used in this work package. Mice that undergo conditional pericyte ablation are produced in our laboratory and are also used in our other studies. To explain the method briefly; It is created by mating mice expressing the Cre-recombinase-estrogen receptor under the control of the PDGFR beta promoter region (PDGFRβ-P2A-CreERT2, The Jackson Laboratory) and mice expressing the attenuated diphtheria toxin gene (Rosa26-DTA176 The Jackson Laboratory). PDGFRβ-CreERT2/Rosa26-DTA176 animals are identified by genotyping and tamoxifen is given when they reach adulthood. Thus, diphtheria toxin is synthesized only in cells containing PDGFRbeta, which is specific to pericytes, and pericyte cells undergo apoptosis when tamoxifen is administered.

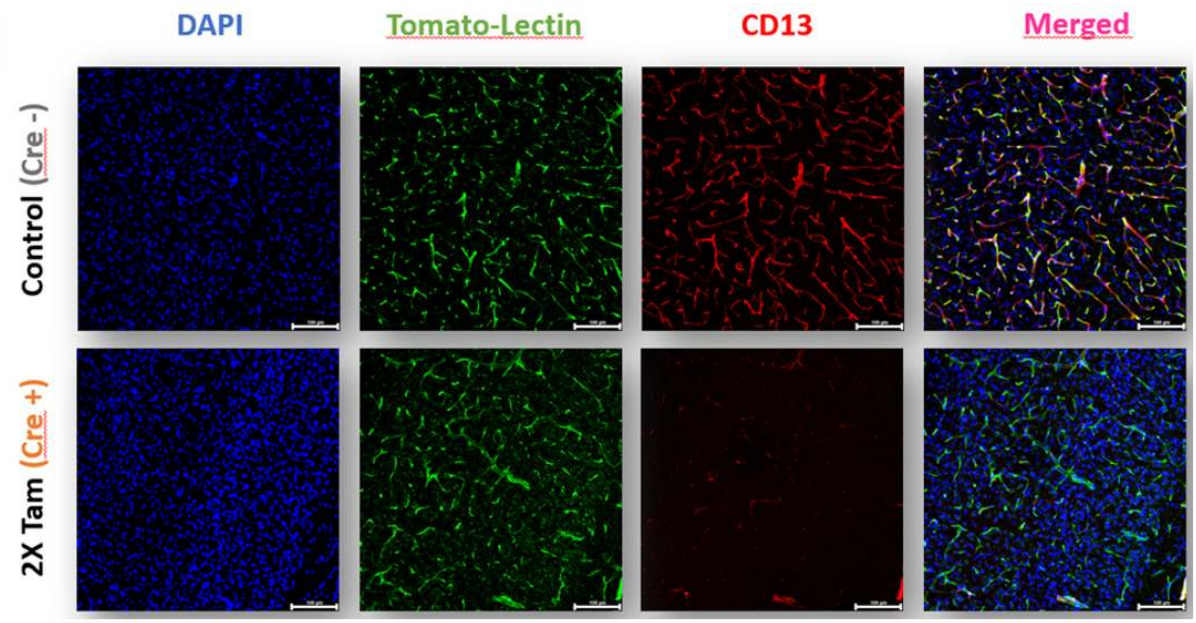

Figure 2.3 shows that CD13-labeled pericytes are largely ablated in the transgenic mouse.

Histological examination shows that CD13+ pericytes disappear around Tomato-Lectin+ vessels in mice given tamoxifen in the pericyte ablation model (b). Animals with CRE = PDGFRβ-P2A-CreERT2 genotype; CRE+ROSA= animals of PDGFRβ-CreERT2/Rosa26-DTA176 genotype; Full=tamoxifen.

Groups	Pericyte Ablated, Hypertensive	Normal Pericyte, Hypertensive	Perisit Ablate, Normotensive	Pericyte Ablated, Hypertensive, Losartan Treatment	Normal Pericyte, Hypertensive, Losartan Treatment
Species	CRE+ROSA	C57	CRE+ROSA	CRE+ROSA	C57
Infusion	AT2	AT2	Saline solution	AT2	Saline solution
Number of subjects	8	8	8	8	8

Figure 2.4 Experimental groups.

2.4. Insertion Of The Osmotic Pump And AT2 Infusion

After the animals reach 10 weeks of age, the back portions are shaved and cleaned using solutions containing 70% alcohol and 2% iodine while they're under a 3-5% isofluorane anesthetic. The subcutaneous tissue to the right of the incision then be enlarged with the aid of hemostatic forceps, an osmotic pump (Alzec, Cupertino, CA) positioned to give continuous AT2 infusion, and an incision created at the left mid-scapular line. The wound then be stitched closed with surgical stitches. After dissolving AT2 (Sigma-Aldrich, MO, USA) in a sterile saline solution, a four-week continuous infusion regimen (1000ng/kg/day) was initiated. In the normal pericyte-normotensive group, the same procedure is repeated, but only an osmotic pump filled with sterile saline is placed. Pain management is carried out in animals by adding paracetamol to their drinking water after the procedure.

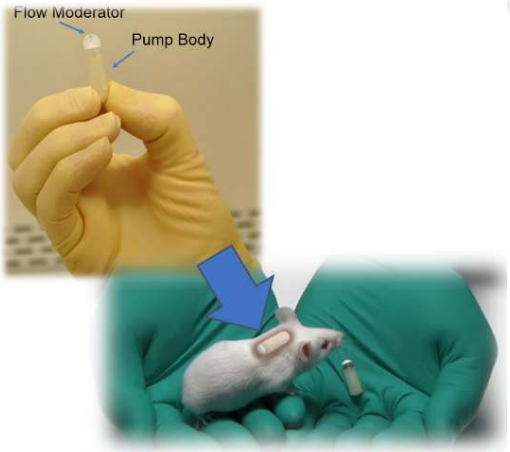

Figure 2.5 Insertion of the osmotic pump in animals

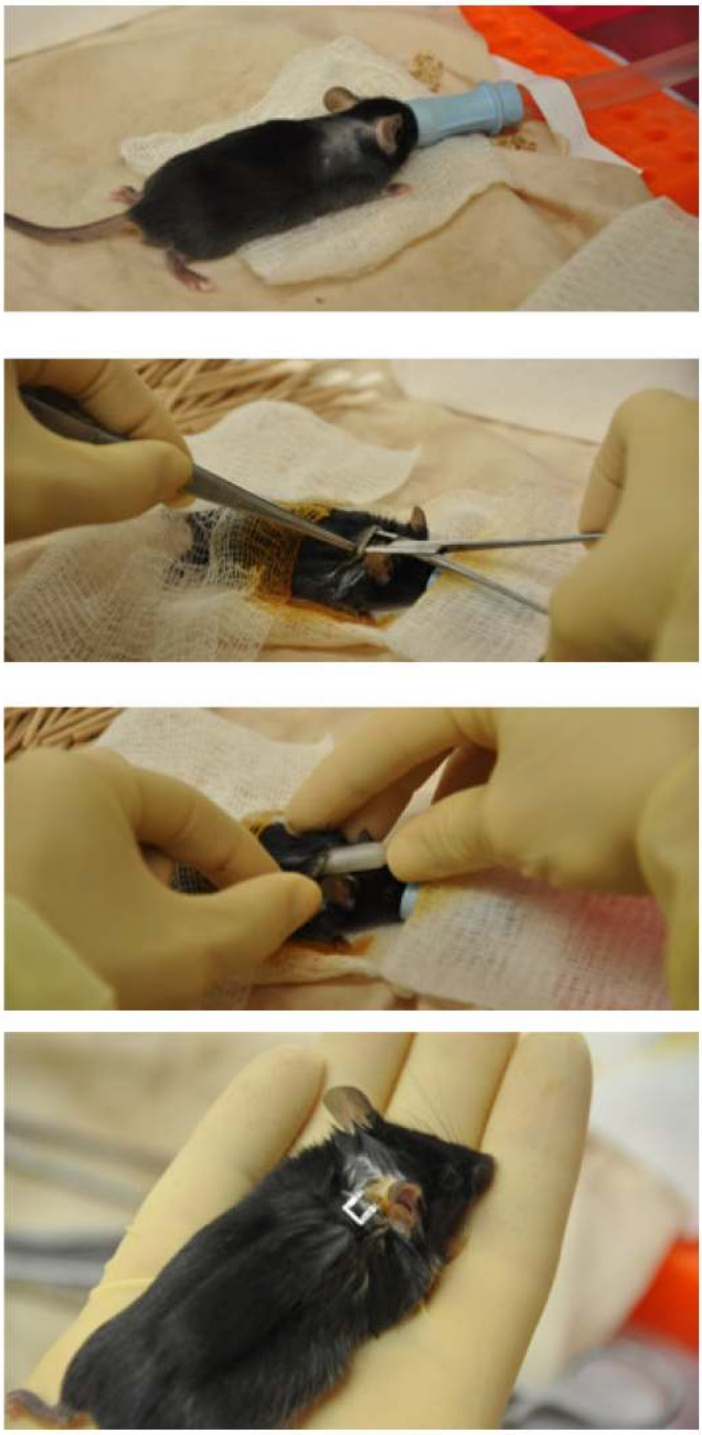

Figure 2.6 Process of pump implantation surgery (Lu et al., 2015).

2.5. Blood Pressure Monitoring

Blood pressure was measured daily prior to the procedure, at the 6th hour, at the 24th hour, and thereafter using a non-invasive manner. The CODA tail-cuff system (Kent Scientific) with a VPR sensor was used for this purpose. Before starting blood pressure measurements, the subjects were placed in a restraint device every day for two weeks and were accustomed to reducing their stress during actual measurements.

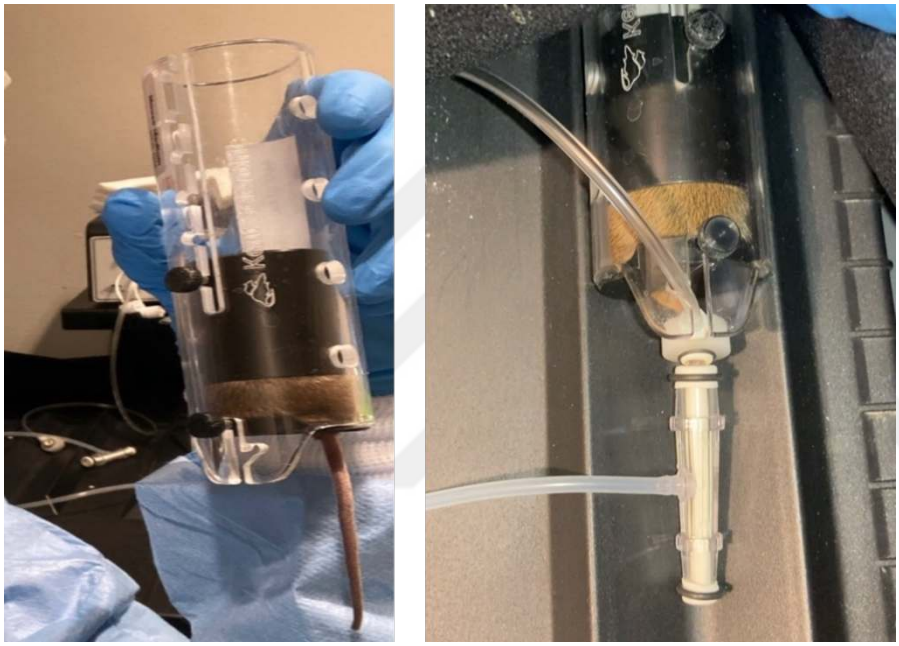

Figure 2.7 Images of the Koda blood pressure monitor.

The animals are placed in a restrainer as seen in the first picture and the device is shortened and locked to prevent them from turning. The tail cuff is placed on the animal's tail as seen in the second picture.

2.6. Treatment Application

In the planned treatment groups, the active substance losartan, an angiotensin receptor blocker, is administered orally. Losartan was added to drinking water (0.9 g/L, Cozaar, Merck) as stated in the literature (Lin et al., 2014). Daily intake is targeted at 3.5ml/day

per subject. The continuation of the treatment is monitored by monitoring the daily drinking water volume in the treatment groups. In the pericyte ablation group, treatment begins with the start of angiotensin 2 infusion and continues for 4 weeks.

2.7. Behavioral Experiments

Behavioral experiments were conducted to detect cognitive impairments that occur in the HT model. Experiments first start when the mice are 12 weeks old and repeated after 4 weeks of AngII infusion. All behavioral experiments were conducted by the same researcher in the same room. In the week before the behavioral experiments, all subjects are accustomed to being taken to the room where the experiment will be performed, taken out of their cages, and handled by the researcher. During the experiments, the experimental setup was cleaned with 70% alcohol solution after each animal.

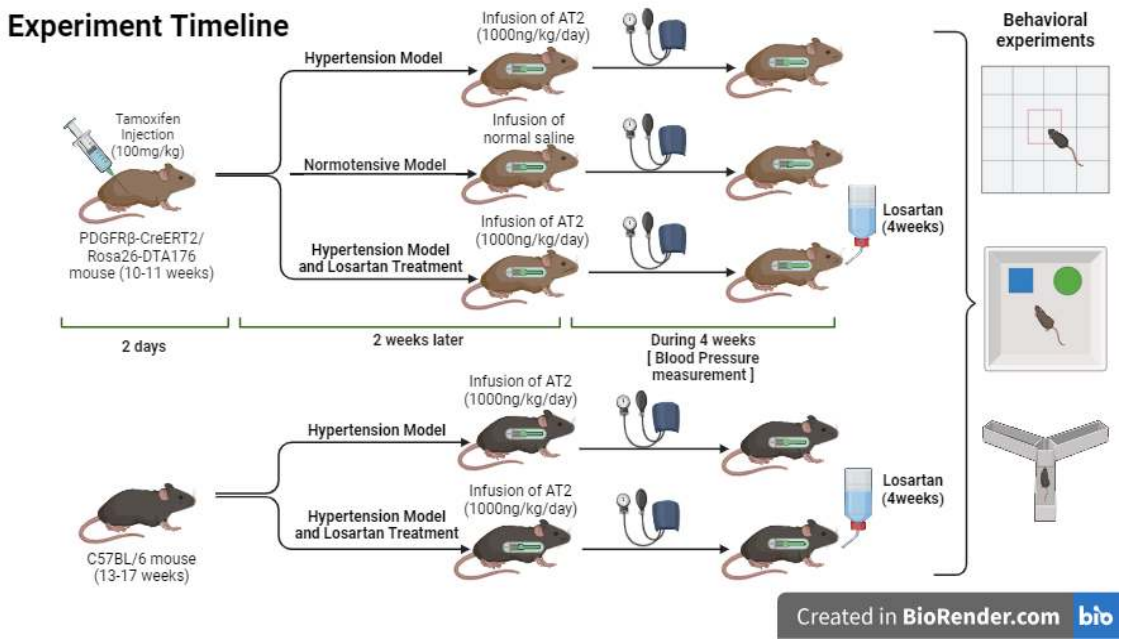

Figure 2.8 Experiment timeline of behavioral experiments.

2.7.1. Open Field Test

The main aim of the open-field locomotor activity test is to detect anxiety-like behavior in animals. This examination is essential for evaluating temporal and spatial memory without disregarding any concerns or anxieties. The literature states that the open field test box used for mice had dimensions of 40x40x40 cm and was made entirely of white plexiglass. Once the subjects are placed in the center of the empty box, a video recording lasting six minutes is created. The Ethovision XT video processing tool was utilized to examine the recorded footage post-experiment in order to ascertain the subjects' overall distance traveled and the duration of time they spent in the central area of the open field box.

Figure 2.9 The Open field test setup.

2.7.2 The Y-Maze Test

The white-colored Y maze, measuring 6 cm in width, 20 cm in depth, and with arm lengths of 35 cm, was used to measure the animals' spatial recognition memory . The mice were observed for a duration of 5 minutes immediately after departing from the center of the maze. The maze was sterilized using a 10% ethanol solution and allowed to air dry before each experiment. The recordings were subsequently viewed and quantified manually. During the quantification process, the three arms were designated as A, B, and C (Figure 2.10). The arm entries were recorded. A spontaneous alteration was defined as sequentially entering all the arms without revisiting any previously visited arms. To calculate the Y maze score, the quotient of the number of spontaneous modifications and the total number of triads was determined.

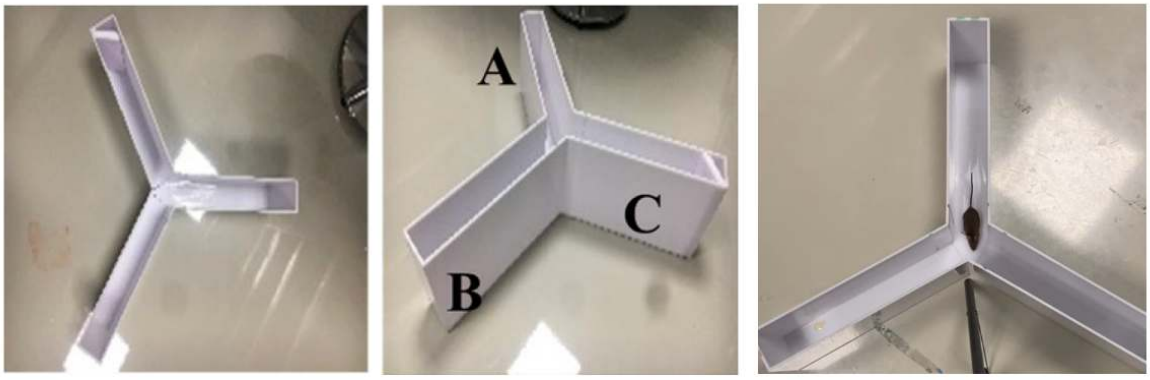

Figure 2.10 The image of the Y maze setup and its labeling for the quantification process was illustrated.

2.7.3 Novel Object Recognition Test

The visual memory test is used to assess new object recognition. The test consists of three distinct parts.

a) Exercise: Animals spend six minutes in the same box that was utilized for the open field test.

b) Pretest: Two identical objects are put in the experimental box for the pretest phase. The subjects are left in the box for ten minutes the day after the exercise, and the entire session is recorded on video. The animals in the experiment who look at the objects for less than 20 seconds will be eliminated at this point.

c) Test: A different used in place of one of the identical objects during the testing phase. The animals were placed in the test box and a 5-minute video recording was made after the pretest phase, which lasts 24 hours for mice. The Ethovision XT program also be used to assess videos taken during the pretest and test periods. Behaviors related to object recognition that include smelling, licking, and touching an object at a maximum distance of 2 cm with the head pointed in its direction are approved in this experiment (Leger et al., 2013). The time spent identifying the new object divided by the total time spent recognizing two objects was used to determine the object identification score after the trial.

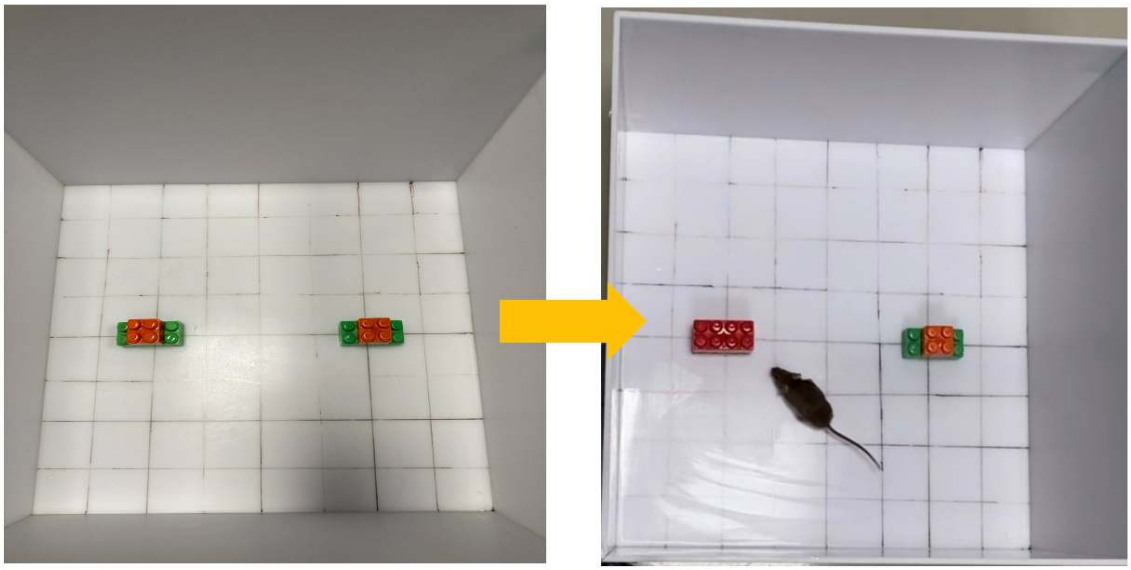

Figure 2.11 The Novel object recognition test setup.

2.8. Injection Of Fluorescently Labeled Amyloid Beta into The Cisterna Magna

Hypertensive mice were placed in a stereotactic frame under isofluorane anesthesia and fluorescently labeled amyloid was injected into the cisterna magna and n=8 animals for each group will be perfused in 45 minutes to examine amyloid clearance. Its departure was monitored.

The protocol is as follows:
Mice were placed in a stereotactic frame under isofluorane anesthesia. The area between the ear retainers and the upper shoulder area is shaved. The occipital crest is identified under the stereomicroscope and a 10 mm skin incision is made in the midline, below the occipital crest. The subcutaneous tissue and occipital muscles separated with the help of blunt-tipped forceps to expose the dura covering the cisterna magna. With the help of a Hamilton syringe, the atlanto-occipital membrane entered at a right angle to the ear stabilizers and pushed until the resistance decreases (cisterna magna). 2 µl- 100 µM Aβ1-40 Hylite Fluor 555 (Bioscience) will be injected over 2.5 minutes. The syringe was left in place without being moved for another 2 minutes. It was removed later. Animals that survive for the period specified in the protocol are perfused as specified for immunofluorescence imaging.

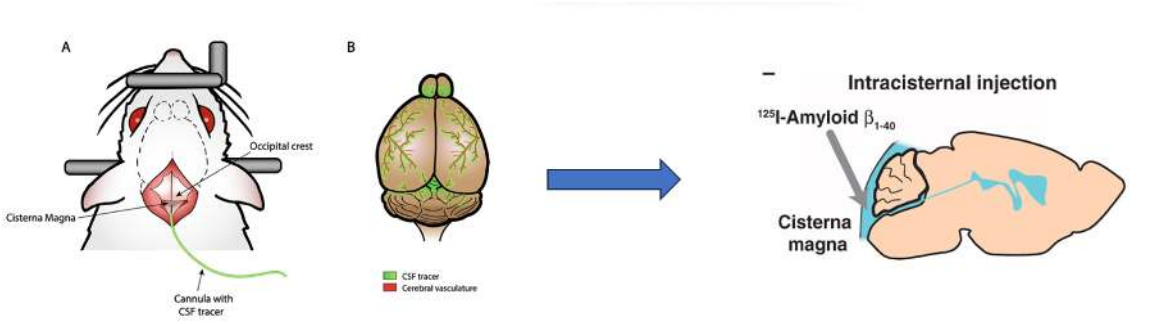

Figure 2.12 The image of injection into cisterna magna.

2.9. Immunofluorescence Imaging in Cryo-Sections

Subjects allocated for IF in the experimental groups were perfused first with saline solution and then with 4% PFA. Cryoprotection was provided by keeping PFA in 10%, 20%, and 30% sucrose solutions at +4 °C until it settles to the bottom. The brains obtained after perfusion were embedded in the cryomatrix by taking 2 mm sections, starting from the frontal. For staining, 30µm sections are taken from the tissues embedded in the cryomatrix and first dipped in distilled water and then kept in 100% methanol for five minutes for permeabilization. After washing with Dulbecco's phosphate buffered saline (DPBS), it will be kept in Superblock (Thermo Scientific™, PI37535) at room temperature for one hour. Primary and secondary antibodies were also prepared in Superblock. Then, primary antibodies were added at the determined dilution and kept at 38 °C for 1.5 hours. After washing with DPBS, the appropriate secondary antibody was kept at 38 °C for 1.5 hours and washed with DPBS. In double staining, this process is repeated for the second primary antibody. The sections then be sealed with 4',6-diamidino-2-phenylindole (DAPI, Abcam), and images taken with fluorescence or confocal microscopy.

2.10. Immunofluorescence of Cryosections Protocol

1) Dip slide in dH_2O a few times to Remove/Melt OCT.
2) Dip slide in methanol and leave for 5 min RT.
3) Wash 3x in DPBS (dipping slide).
4) 10 min in microwave in citrate buffer.
   Citrate buffer: Antigen Retriveval 1ml+99ml ddH_2O (1:100)
5) Washing with water for 5 minutes after cooling.
6) Permeabilization for 10 min at room temperature.
   Permeabilization: 1 ml Triton-X-100 + 9ml ddH_2O (**main stock 10% Triton-X**)

Usage stock (1:100)
1 ml main stock Triton-X + 99ml DPBS

7) Add block buffer (superblock in common fridge +4°C) to each sample on slide (First make a circle with pappen) and incubate at RT for 1 hour (humidified).
8) Remove superblock and add primary antibody of interest to each sample and incubate overnight at +4°C.
9) Collect primary ab for Re-use.
10) Wash slides 3x in DPBS by dipping for 1-2 min.
11) Add secondary antibody of interest to each sample and incubate 1,5 hour at 37°C in (dark and humidified).
12) Remove and secondary ab.
13) Wash 3x with DPBS.
14) Mount with DAPI.
15) Leave for 10 min to dry.
16) Visualize with microscopy.

2.11 Statistical Analysis

GraphPad Prism 10 (San Diego, USA) was used for all statistical analyses. Data were presented as Mean±SD if not mentioned otherwise. The Shapiro-Wilk normality test was used to make normality assumptions. The groups were compared using the Kruskal-Wallis test. The Mann-Whitney U test was employed to compare the two groups. P-values ≤ 0.05 were considered significant.

Chapter 3

RESULTS

3.1. Animals

According to genotyping analysis, 28 CreER-positive animals were identified. Animals between the ages of 10 and 11 weeks were chosen for the purpose of creating the model. The pump procedure was conducted two weeks after administering tamoxifen injections, when the mice reached 13 weeks of age. Only one of the 28 pericyte-ablated animals died on the third day of tamoxifen injections. The death rate attributed to tamoxifen injections was determined to be 4%. In the group of 24 pericyte-ablate animals that received ATII infusion, 2 also died by the end of the second week (ATII-related mortality was 8.3%). The control group consisted of 16 C57BL/6 mice, aged between 13 and 17 weeks, purchased from the Koç University Laboratory Animal Center. The control group did not experience any deaths associated with the operation of the pump or the infusion of ATII. The animals' weights were regularly examined on a weekly basis, and by the end of the trial, their weights were comparable to the original values.

3.2. Blood Pressure Measurements

Before the surgery, blood pressure measures were taken using the CODA equipment to acquire normotensive data. Following the operation, blood pressure was assessed on days 7, 14, 21, and 28 to evaluate the transition to hypertension. The CODA tail-cuff system utilizes volume pressure recording (VPR) to measure blood pressure by assessing the blood volume in the tail. A

specifically engineered differential pressure transducer and occlusion tail cuff are used to quantify the overall blood volume in the tail, eliminating the requirement for acquiring individual pulse signals. The CODA system offers precise measurements of both systolic and diastolic blood pressure parameters. The laboratory where the CODA device is utilized must maintain a minimum room temperature of 20°C or greater. Animals were placed in pairs and confined in restrainers. The CODA tail-cuff equipment was connected to the tails externally, while they were held in the restrainers. Measurements were conducted within a time frame of 15 minutes, ensuring that the animals were not confined in the restrainer for an extended period. With the exception of the pericyte-ablate normotensive group, all animals exhibited a considerable increase in blood pressure when compared to their initial values (Figure 3.1).

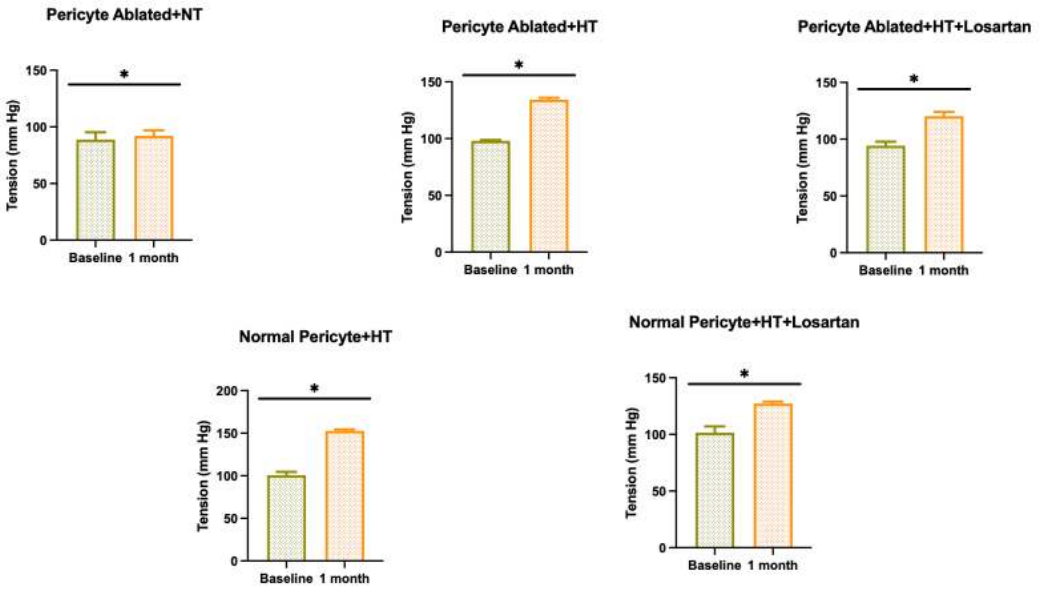

Figure 3.1 Blood pressure values of animals on the first and last day.

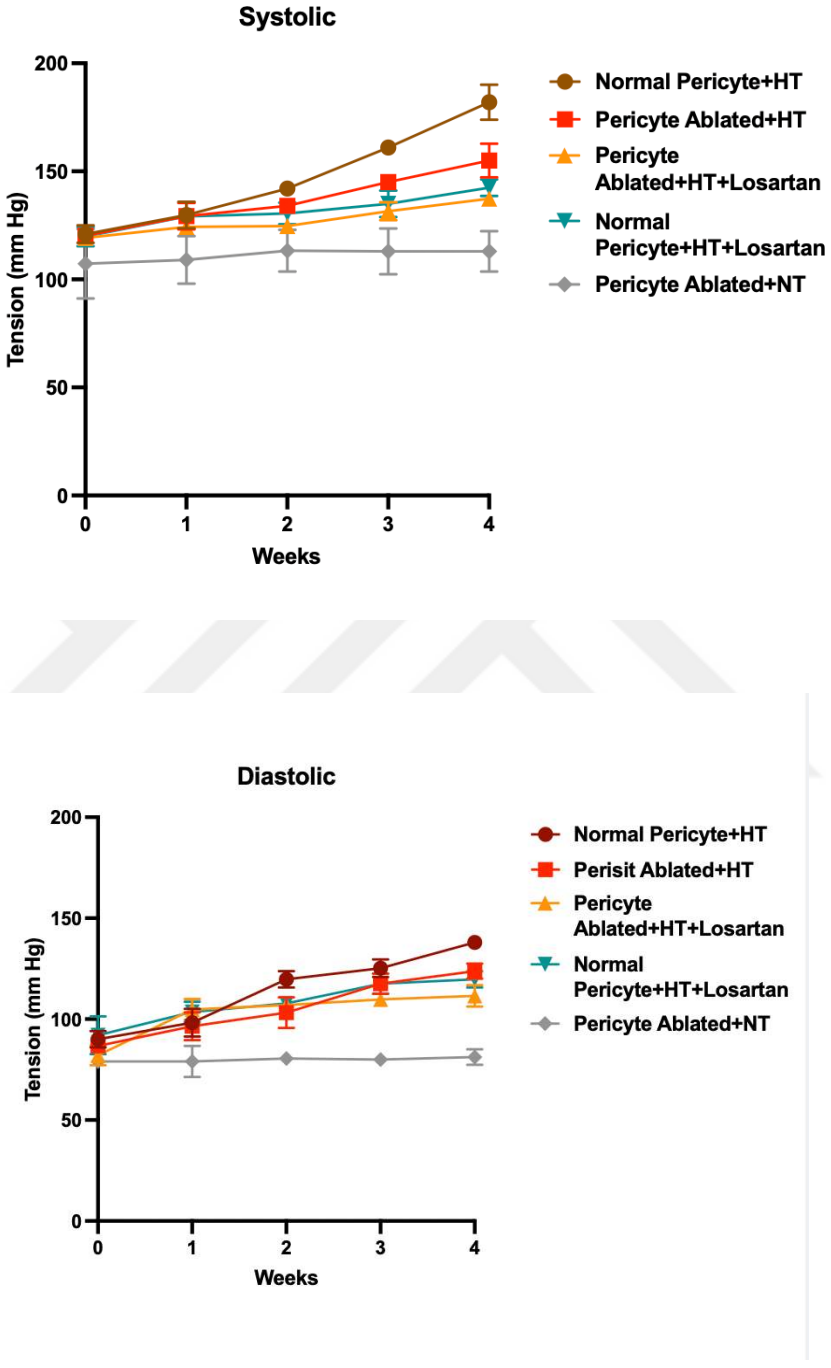

Figure 3.2 Systolic and diastolic blood pressure measurements of animals.

Pericyte ablated and non-pericyte ablated animals became hypertensive after ATII infusion. Blood pressure measurements tended to be lower in the pericyte ablated groups.

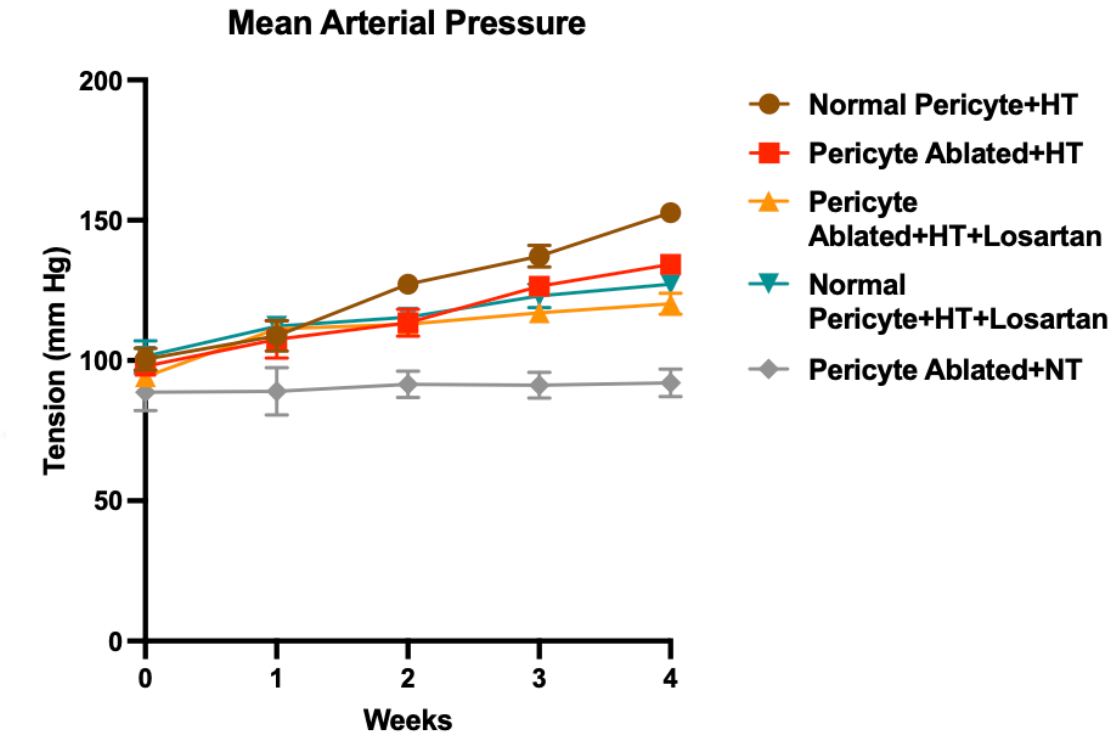

Figure 3.3 Animal mean arterial pressure measurements.

The mean arterial pressure is obtained by adding twice the diastolic pressure to the systolic pressure and then dividing the sum by 3.

3.3. Behavioral Experiments

In order to detect cognitive and motor changes due to hypertension, behavioral tests were applied to all animals in the last week. All behavioral experiments were performed by the same researcher in the same room. In the week before the behavioral experiments, all subjects were accustomed to being taken to the room where the experiment would be performed, taken out of their cages and held by the researcher. During the experiments, the experimental setup was cleaned with 70% alcohol solution after each animal.

3.3.1. Open Field Test

The open field locomotor activity test was designed to reveal anxiety-like behavior in subjects. This test is important for evaluating temporal and spatial memory tests independently of anxiety effects. The dimensions of the open field test box made entirely of white Plexiglas were determined as 40x40x40 cm for mice as described in the literature. 64 squares of 5x5 cm were drawn inside the box. The subjects were placed in the middle of the empty box and a video recording lasting 5 minutes was taken. At the end of the experiment, the video was manually analyzed in terms of the total line covered by the animals.

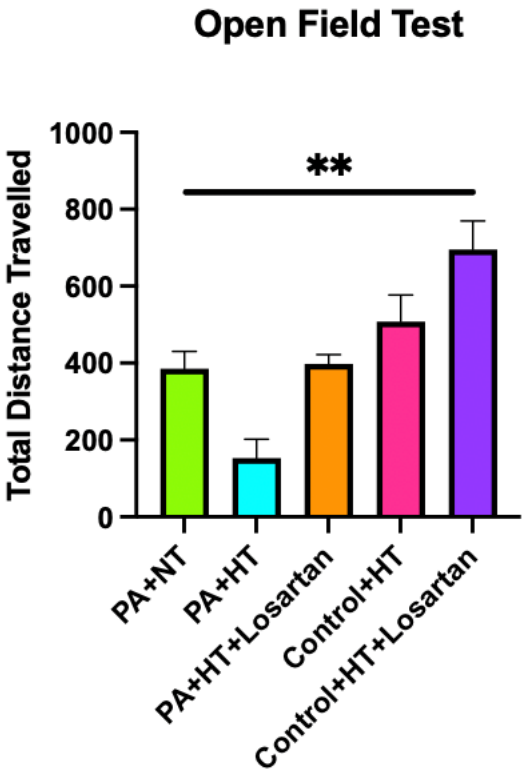

Figure 3.4 Results of the open field test.

The groups in which pericytes were ablated showed a significant decrease in the total number of squares covered, as compared to the groups with normal pericytes.

3.3.2. Y Maze Test

The Y-maze test was chosen to provide an idea about the working memory of the animals. A setup consisting of 3 closed arms and a center, placed at an angle of 120 degrees, was used in the experiment. The dimensions of the arms of the Y-maze were 20x40x10cm. The animals were left in the center of the maze and video recording was made for 5 minutes. At the end of the experiment, the spontaneous alternation index, which gives an idea about whether the animal has memorized the arm it entered before, was calculated.

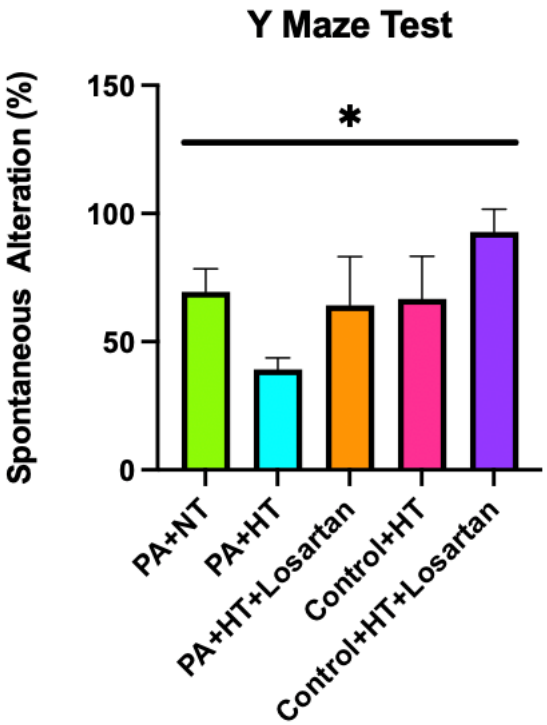

Figure 3.5 Y maze test.

3.3.3. Novel Object Recognition Test

The novel object recognition test was used to assess visual memory. The test consisted of 3 stages.

a) Practice: Animals were left in the box used for the open field test for 5 minutes.

b) Pretest: For the pretest stage, two identical objects were placed in the experimental box and 24 hours after the practice, the subjects were left in the box for 10 minutes and the session was videotaped.

c) Test: In the test stage, one of the identical objects was replaced with a different object. 6 hours after the pretest stage, the animals were placed in the test box and a 5-minute video recording was taken. At the end of the experiment, a discrimination score was calculated for each animal. The score was calculated as the time spent examining the novel object (object sniffing, licking, touching the object from a distance of up to 2 cm with the head turned towards the object) measured from the video taken during the test stage, divided by the total time spent examining both objects.

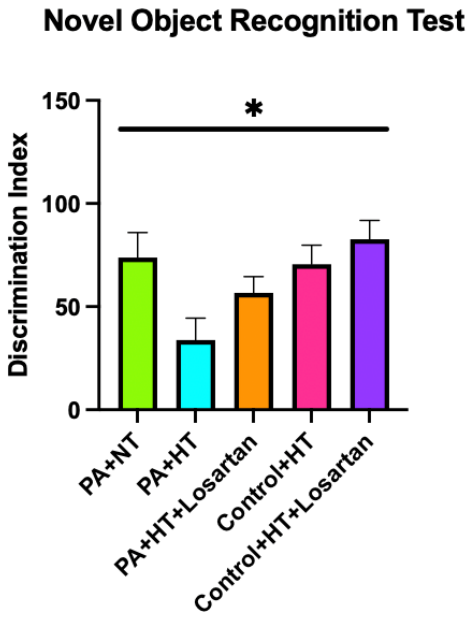

Figure 3.6 Novel object recognition test.

3.4. Injection Of Fluorescently Labeled Amyloid Beta into The Cisterna Magna

For the injection of fluorescently labeled amyloid beta into the cisterna magna, mice were placed in a stereotactic frame under isoflurane anesthesia. The area between the ear fixators and the upper shoulder region were shaved. The occipital crest was identified under the stereomicroscope and a 10 mm skin incision was made in the midline, below the occipital crest. The subcutaneous tissue and occipital muscles were separated with blunt-tipped forceps to expose the dura covering the cisterna magna. The atlanto-occipital membrane was entered at a right angle to the ear fixators with the help of a Hamilton syringe and pushed until the resistance decreased (cisterna magna). 2 µl - 100 µM Aβ1-40 Hylite Fluor 555 (Bioscience) was injected within 2.5 minutes. The syringe was kept in place without moving for another 2 minutes. The animals were perfused after waiting for 45 minutes.

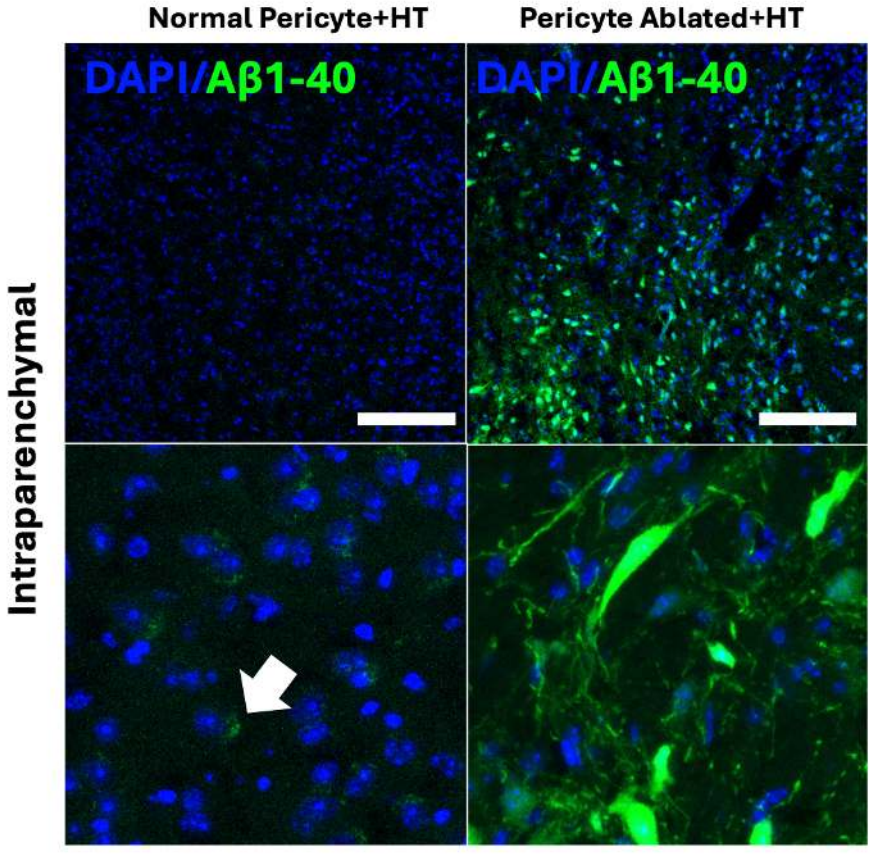

Figure 3.7 Comparison of Aβ1-40 clearance in intraparenchymal areas between pericyte ablated and normal pericyte hypertension groups.

At 45 minutes after injection, fluorescent amyloid beta showed a distinct intraparenchymal distribution in the pericyte ablated group. In the zoomed images in the bottom row, there was a trace amount of fluorescently labeled amyloid in the normal pericyte group (white arrow), while it was clearly observed in the pericyte ablated group.

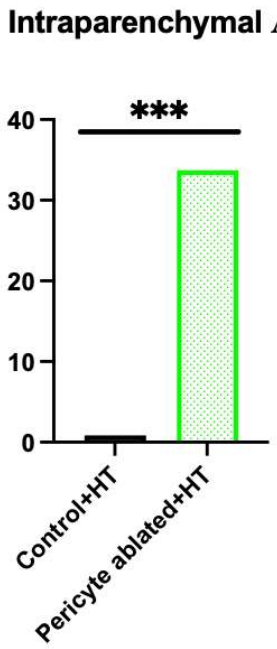

Figure 3.8 The analysis of Amyloid-β images among Pericyte-ablated hypertensive and Control hypertensive groups

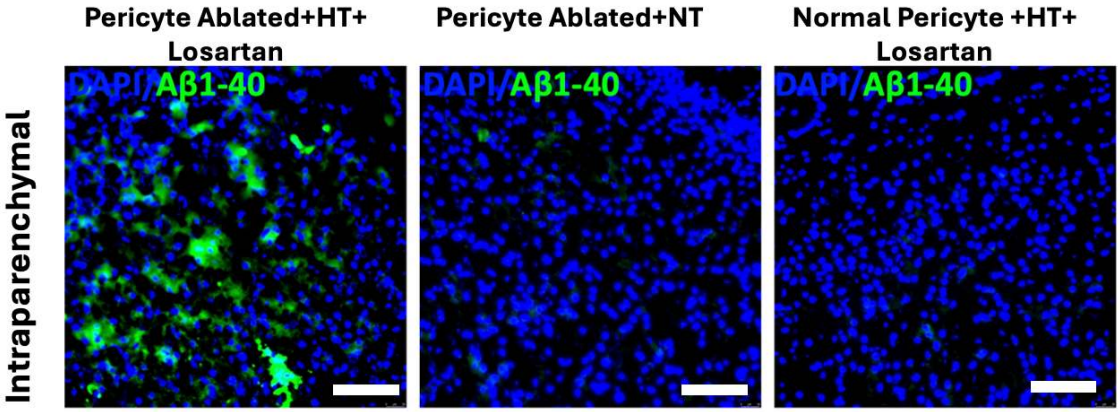

Figure 3.9 Comparison of intraparenchymal fluorescent marker.

At 45 minutes after injection, fluorescent amyloid accumulation was observed in the pericyte ablation normotensive group due to blood-brain barrier disruption. In the

group of pericyte ablation hypertension treatment group, there is a higher accumulation of amyloid compared to the group of normal pericyte treatment group.

While fluorescent amyloid beta showed a distinct intraparenchymal distribution in the pericyte ablated hypertensive group 45 minutes after injection, it was not observed in the veins of pericyte ablated hypertensive animals (Figure 3.10). When the intraparenchymal area was examined, there was a small amount of fluorescently labeled amyloid in the normal pericyte hypertensive group. However, it was observed that amyloid accumulation was still dense in the veins (Figure 3.10). It was observed that AF 488-labeled Aβ1-40 injected into the cisterna magna was completely cleared from the ventricles in both groups 45 minutes after injection (Figure 3.11).

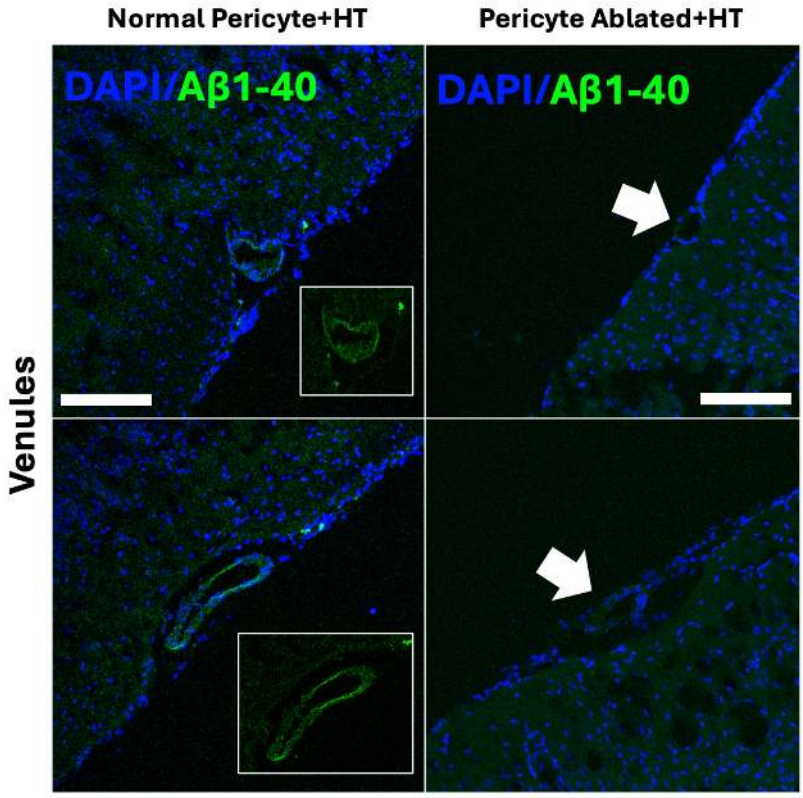

Figure 3.10 Comparison of fluorescently labeled amyloid in pial veins.

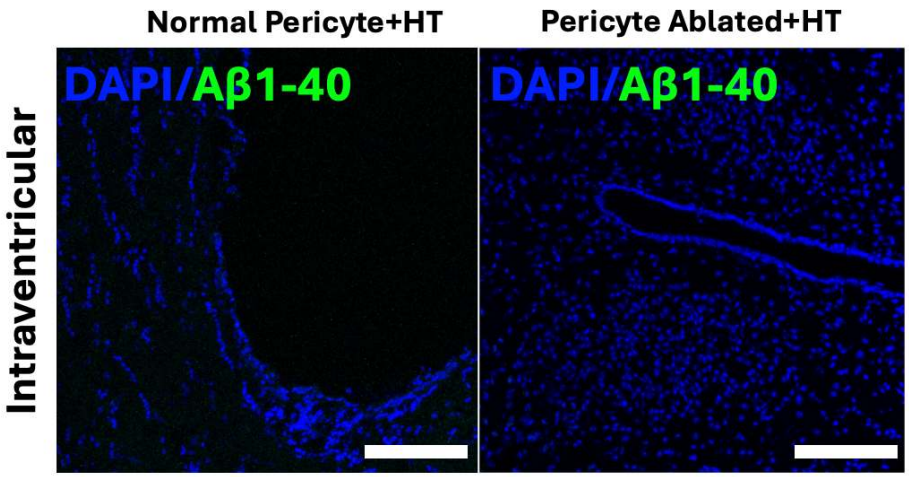

Figure 3.11 Intraventricular fluorescent marker screening.

3.5. NeuN Staining results

The number of neurons is decreased in neurodegenerative diseases. We stained frozen sections with NeuN antibody to show the number of neurons between groups. As expected, the percentage of NeuN stained area between groups was similar in the hippocampus when AF488-labeled Aβ1-40 was injected into the cisterna magna and perfused 45 min after injection.

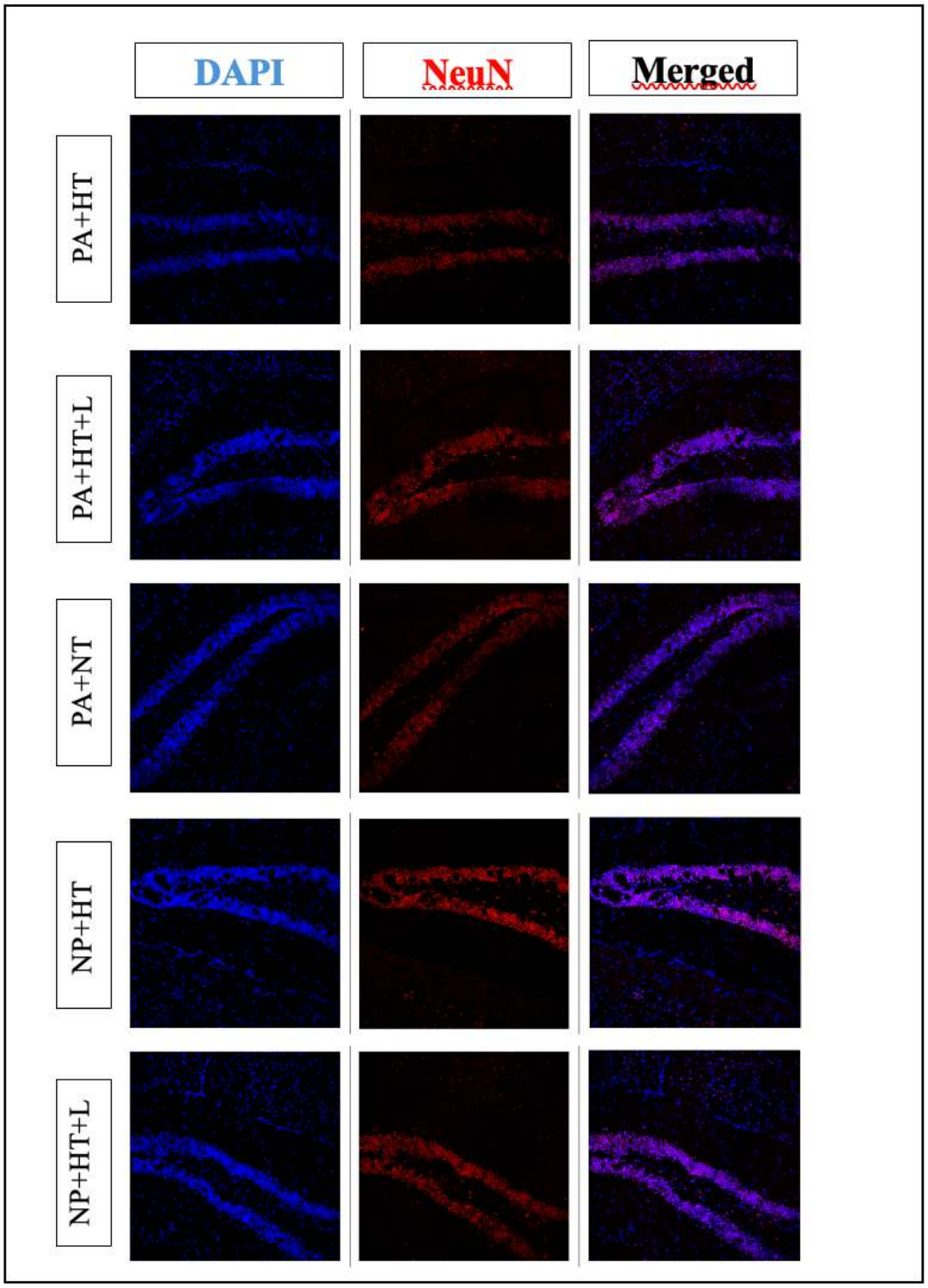

Figure 3.12 Neun staining for all groups. The Neun-stained area is similar between groups in the hippocampus. The scale bar is 100μm.

The Neun-stained area was lowest in the pericyte-ablated groups due to blood-brain barrier damage in the hippocampus. However, this change did not reach statistical significance.

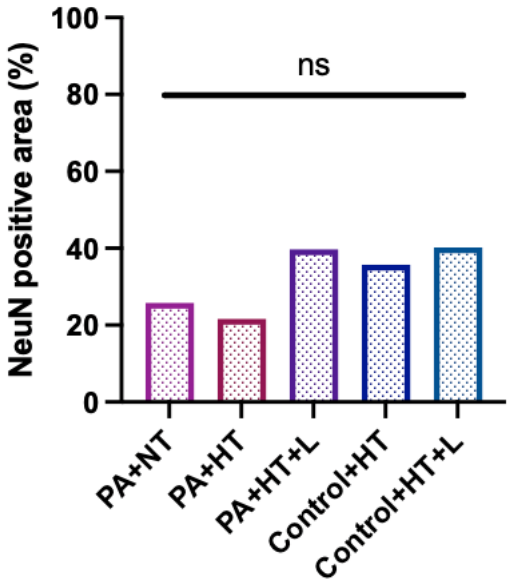

Figure 3.13 The analyses of NeuN stained images among groups.

Chapter 4

DISCUSSION

The decline in cognitive function and the rise in dementia rates that come with aging are significant issues that are brought on by the average life expectancy in society increasing. Clinical research has indicated that white matter lesions, small artery disease, and occlusions in deep brain vessels all worsen with age and are major contributors to declining cognitive function.

Chronic hypertension is the primary risk factor for stroke and cerebrovascular impairment. Studies on this topic that are population-based have shown a causal link between cognitive decline and hypertension. Once more, comparable research shows a robust correlation between white matter lesion burden and hypertension and brain imaging (MRI) (Pasi and Cordonnier, 2020). By 2025, 50% of Americans, according to the American Heart Association, will have hypertension. It is reasonable to anticipate that this percentage will be comparable to or higher in other nations, particularly in our own, where hypertension is a major issue. Examination of patients with hypertension revealed a strong correlation with cerebral small vessel disease, and 80% of those over 60 who had an MRI showed lesions resembling small vessel disease, regardless of their status as hypertensive patients. (Gurol, Biessels, and Polimeni, 2020) It suggests that hypertension-related cognitive impairment may be significantly impacted by alterations in the brain microvascular bed and changes that disrupt functional blood flow regulation. The build-up of extracellular matrix elements including collagen and fibronectin in the brain microcirculation is a consequence of hypertension, according to postmortem investigations. Arteriosclerosis results from this pathogenic process, which is known as hypertrophic remodeling.

Clinical evidence indicates that these alterations are linked to cognitive decline and silent lesion load, particularly in hypertensive individuals (Østergaard et al., 2016). In this study, we aimed to investigate the effects of pericytes on blood pressure values, disease course, cognition and brain fibrosis and waste material clearance by triggering HT in a transgenic pericyte ablation mouse model. In this section, we will go over our main conclusion and its possible implications.

To investigate the role of pericyte-fibrosis-microcirculation-neurodegeneration content in hypertension-associated cerebral small vessel disease, pericyte conditional ablation normotensive-hypertensive and treatment groups and normal pericyte hypertensive-treatment groups were created. We included 28 CreER-positive transgenic mice and 16 C57BL/6 mice as control groups in our experiments. The overall mortality of the surgery was 8.3% for transgenic mice. The animals were subjected to 4 weeks (chronic), high-dose AT2 infusion model. This is because this dose has been reported to cause cognitive changes, blood brain barrier damage, hypertrophic response in organs and vascular remolding (Lerman et al., 2019). Before the procedure, the animals had their blood pressure measured with the CODA device for normotensive data, and after the procedure, their blood pressure was measured on the 7th, 14th, 21st and 28th days to show the hypertensive transition. The blood pressure values measured before the experiment increased compared to the beginning for all groups (except the pericyte ablated normotensive group). However, the blood pressure values of the animals in the normal pericyte hypertension group were higher than those in the pericyte ablated hypertension group. Pericyte ablation causes blood pressure values to be lower in the HT model.

Openfield, y maze, and new object recognition test behavioral experiments were performed to detect cognitive disorders in the HT model. Open field locomotor activity test was designed to reveal anxiety-like behavior in subjects. According to the open field test results, the number of squares passed was the least in the Pericyte ablated group, while it was the most in the normal pericyte hypertensive losartan treated group. We chose the Y-maze test to give an idea about the subjects' working memory. At the end of the experiment, the spontaneous alternation index, which gives an idea about whether the animal keeps the

previous arm it entered in its memory, was calculated. The spontaneous alternation index of the Pericyte ablated hypertensive group was the lowest. Novel object recognition test was used to measure hippocampus-dependent short-term visual memory. When the novel object discrimination indexes were evaluated, the worst result was again the data of the Pericyte ablated hypertensive group.

The hypothesis of our study was to demonstrate that hypertension-related cerebral small vessel disease involves an additional mechanism that impairs the clearance of metabolic waste products from the brain, including amyloid beta associated with pericytes in the vascular wall, thus leading to cognitive impairment. Animals were perfused 45 minutes after the injection of fluorescently labeled amyloid beta into the cisterna magna. The clearance of Aβ1-40 between groups was compared by monitoring the intraventricular fluorescent marker in the pial arteries, intraparenchymal, and venules. To examine the clearance mechanism of metabolic waste products, we first looked inside the ventricle and proved that amyloid was no longer deposited in the ventricle. When we looked at the parenchyma, we saw that amyloid was dramatically distributed in the parenchyma in the pericyte-ablated hypertensive group. Amyloid was not observed in the parenchyma for the non-pericyte ablated groups. However, while amyloid reached the vein in the non-pericyte ablated hypertensive group, it was not observed around the vein in the ablated hypertensive group. We think that amyloid cleared from the parenchyma and reached the vein after 45 minutes in the normal pericyte group, while amyloid accumulated in the parenchyma in the ablated group, which indicates that the clearance pathway is not working. We also think that it is associated with significant locomotor slowness, delayed Aβ clearance, and intraparenchymal accumulation.

NeuN protein is localized in the nuclei and perinuclear cytoplasm of most neurons in the mammalian central nervous system. Monoclonal antibodies to NeuN protein have been actively used for more than 20 years in immunofluorescence studies of neuronal differentiation to assess the functional status of neurons in terms of norm and pathology (Gusel'Nikova et al., 2015). Our study examined the effects of amyloid accumulation on neurons when brain waste clearance

pathways are not working. The Neun-stained area was lowest in the pericyte-ablated groups due to blood-brain barrier damage in the hippocampus. However, this change did not reach statistical significance. Considering the results, we think there is no significant change in neurons because we examined the early effects of amyloid accumulation.

Chapter 5

CONCLUSION

In this thesis project, we aimed to investigate the effects of pericytes on microcirculation, cognition, neurodegeneration, and waste product clearance by inducing HT in a transgenic pericyte ablation mouse model. We hypothesized that there is an additional mechanism that disrupts the clearance of metabolic waste products from the brain due to pericytes, thus leading to cognitive impairment. We also included transgenic pericyte ablation groups to specifically examine the role of pericytes in the experimentally induced hypertension model. According to our aim, we injected fluorescently labeled beta-amyloid into the cisterna magna of mice that underwent chronic AT2 infusion. In our study, cognitive profiles were checked with a series of behavioral tests performed one month later. In parallel with our hypothesis, the pericyte-ablated hypertensive group showed worse behavioral test performance than all other groups. According to the results of behavioral experiments, this is the first study to show that the significant locomotor slowness in the pericyte-ablated hypertensive group leads to cognitive decline due to delayed Aβ clearance and intraparenchymal accumulation. Consistent with all of this data, healthy pericytes may be of critical importance in clearing toxic substances from the brain in the setting of HT and protecting against dementia.

BIBLIOGRAPY

Abbott, N. J., Rönnbäck, L., & Hansson, E. (2006). Astrocyte–endothelial interactions at the blood–brain barrier. Nature reviews neuroscience, 7(1), 41-53.

Achariyar, T. M., Li, B., Peng, W., Verghese, P. B., Shi, Y., McConnell, E., ... & Deane, R. (2016). Glymphatic distribution of CSF-derived apoE into brain is isoform specific and suppressed during sleep deprivation. Molecular neurodegeneration, 11, 1-20.

Asgari, M., De Zélicourt, D., & Kurtcuoglu, V. (2016). Glymphatic solute transport does not require bulk flow. Scientific reports, 6(1), 38635.

Bugiani, M., Kevelam, S. H., Bakels, H. S., Waisfisz, Q., Ceuterick-de Groote, C., Niessen, H. W., ... & Van Der Knaap, M. S. (2016). Cathepsin A–related arteriopathy with strokes and leukoencephalopathy (CARASAL). Neurology, 87(17), 1777-1786.

Cannistraro, R. J., Badi, M., Eidelman, B. H., Dickson, D. W., Middlebrooks, E. H., & Meschia, J. F. (2019). CNS small vessel disease: a clinical review. *Neurology*, *92*(24), 1146-1156.

Caplan, L. R. (2015). Lacunar infarction and small vessel disease: pathology and pathophysiology. Journal of stroke, 17(1), 2.

Chojdak-Lukasiewicz, J., Dziadkowiak, E., Zimny, A., & Paradowski, B. (2021). Cerebral small vessel disease: a review. Adv Clin Exp Med 30: 349–356.

De Ciuceis, C., Cornali, C., Porteri, E., Mardighian, D., Pinardi, C., Fontanella, M. M., ... & Gasparotti, R. (2014). Cerebral small-resistance artery structure and cerebral blood flow in normotensive subjects and hypertensive patients. *Neuroradiology*, *56*, 1103-1111.

De Guio, F., Mangin, J. F., Duering, M., Ropele, S., Chabriat, H., & Jouvent, E. (2015). White matter edema at the early stage of cerebral autosomal-dominant arteriopathy with subcortical infarcts and leukoencephalopathy. Stroke, 46(1), 258-261.

De Leeuw, F. E., de Groot, J. C., Achten, E., Oudkerk, M., Ramos, L. M. P., Heijboer, R., ... & Breteler, M. M. B. (2001). Prevalence of cerebral white matter lesions in elderly people: a population based magnetic resonance imaging study. The Rotterdam Scan Study. Journal of Neurology, Neurosurgery & Psychiatry, 70(1), 9-14.

Duering, M., Csanadi, E., Gesierich, B., Jouvent, E., Herve, D., Seiler, S., ... & Dichgans, M. (2013). Incident lacunes preferentially localize to the edge of white matter hyperintensities: insights into the pathophysiology of cerebral small vessel disease. Brain, 136(9), 2717-2726.

Feekes, J. A., Hsu, S. W., Chaloupka, J. C., & Cassell, M. D. (2005). Tertiary microvascular territories define lacunar infarcts in the basal ganglia. Annals of neurology, 58(1), 18-30.

Fisher, C. M. (1982). Lacunar strokes and infarcts: a review. *Neurology*, *32*(8), 871-871.

Gaberel, T., Gakuba, C., Goulay, R., De Lizarrondo, S. M., Hanouz, J. L., Emery, E., ... & Gauberti, M. (2014). Impaired glymphatic perfusion after strokes revealed by contrast-enhanced MRI: a new target for fibrinolysis?. Stroke, 45(10), 3092-3096.

Ghosh, M., Balbi, M., Hellal, F., Dichgans, M., Lindauer, U., & Plesnila, N. (2015). Pericytes are involved in the pathogenesis of cerebral autosomal dominant arteriopathy with subcortical infarcts and leukoencephalopathy. Annals of neurology, 78(6), 887-900.

Gurol, M. E., Biessels, G. J., & Polimeni, J. R. (2020). Advanced neuroimaging to unravel mechanisms of cerebral small vessel diseases. Stroke, 51(1), 29-37.

Gusel'Nikova, V. V., & Korzhevskiy, D. (2015). NeuN as a neuronal nuclear antigen and neuron differentiation marker. *Acta Naturae (англоязычная версия)*, *7*(2 (25)), 42-47.

Gürsoy-Özdemir, Y., & Tas, Y. C. (2017). Anatomy and Physiology of the Blood–brain Barrier. In Nanotechnology methods for neurological diseases and brain tumors (pp. 3-13). Academic Press.

Hainsworth, A. H., Oommen, A. T., & Bridges, L. R. (2015). Endothelial cells and human cerebral small vessel disease. Brain Pathology, 25(1), 44-50.

Hakim, A. M. (2019). Small vessel disease. *Frontiers in neurology*, *10*, 453063.

Hartmann, D. A., Underly, R. G., Grant, R. I., Watson, A. N., Lindner, V., & Shih, A. Y. (2015). Pericyte structure and distribution in the cerebral cortex revealed by high-resolution imaging of transgenic mice. Neurophotonics, 2(4), 041402-041402.

Hilal, S., Mok, V., Youn, Y. C., Wong, A., Ikram, M. K., & Chen, C. L. H. (2017). Prevalence, risk factors and consequences of cerebral small vessel diseases: data from three Asian countries. Journal of Neurology, Neurosurgery & Psychiatry, 88(8), 669-674.

Huisa, B. N., Caprihan, A., Thompson, J., Prestopnik, J., Qualls, C. R., & Rosenberg, G. A. (2015). Long-term blood–brain barrier permeability changes in Binswanger disease. Stroke, 46(9), 2413-2418.

Iadecola, C. (2017). The neurovascular unit coming of age: a journey through neurovascular coupling in health and disease. Neuron, 96(1), 17-42.

Iadecola, C. (2017). The neurovascular unit coming of age: a journey through neurovascular coupling in health and disease. Neuron, 96(1), 17-42.

Iliff, J. J., & Nedergaard, M. (2013). Is there a cerebral lymphatic system?. Stroke, 44(6_suppl_1), S93-S95.

Inoue, Y., Shue, F., Bu, G., & Kanekiyo, T. (2023). Pathophysiology and probable etiology of cerebral small vessel disease in vascular dementia and Alzheimer's disease. Molecular neurodegeneration, 18(1), 46.

Jiang, Q., Zhang, L., Ding, G., Davoodi-Bojd, E., Li, Q., Li, L., ... & Zhang, Z. (2017). Impairment of the glymphatic system after diabetes. Journal of Cerebral Blood Flow & Metabolism, 37(4), 1326-1337.

Khan, U., Porteous, L., Hassan, A., & Markus, H. S. (2007). Risk factor profile of cerebral small vessel disease and its subtypes. Journal of Neurology, Neurosurgery & Psychiatry, 78(7), 702-706.

Kim, H., Yun, C. H., Thomas, R. J., Lee, S. H., Seo, H. S., Cho, E. R., ... & Shin, C. (2013). Obstructive sleep apnea as a risk factor for cerebral white matter change in a middle-aged and older general population. Sleep, 36(5), 709-715.

Kress, B. T., Iliff, J. J., Xia, M., Wang, M., Wei, H. S., Zeppenfeld, D., ... & Nedergaard, M. (2014). Impairment of paravascular clearance pathways in the aging brain. Annals of neurology, 76(6), 845-861.

Launer, L. J., Hughes, T. M., & White, L. R. (2011). Microinfarcts, brain atrophy, and cognitive function: the Honolulu Asia aging study autopsy study. Annals of neurology, 70(5), 774-780.

Li, Y., Li, M., Zuo, L., Shi, Q., Qin, W., Yang, L., ... & Hu, W. (2018). Compromised blood–brain barrier integrity is associated with total magnetic resonance imaging burden of cerebral small vessel disease. Frontiers in neurology, 9, 221.

Lin, C. H., Yang, H., Xue, Q. L., Chuang, Y. F., Roy, C. N., Abadir, P., & Walston, J. D. (2014). Losartan improves measures of activity, inflammation, and oxidative stress in older mice. *Experimental gerontology*, *58*, 174-178.

Liu, B., Lau, K. K., Li, L., Lovelock, C., Liu, M., Kuker, W., & Rothwell, P. M. (2018). Age-specific associations of renal impairment with magnetic resonance imaging markers of cerebral small vessel disease in transient ischemic attack and stroke. Stroke, 49(4), 899-904.

Lu, H., Howatt, D. A., Balakrishnan, A., Moorleghen, J. J., Rateri, D. L., Cassis, L. A., & Daugherty, A. (2015). Subcutaneous angiotensin II infusion using osmotic pumps induces aortic aneurysms in mice. *JoVE (Journal of Visualized Experiments)*, (103), e53191.

Lundgaard, I., Li, B., Xie, L., Kang, H., Sanggaard, S., Haswell, J. D., ... & Nedergaard, M. (2015). Direct neuronal glucose uptake heralds activity-dependent increases in cerebral metabolism. Nature communications, 6(1), 6807.

Malik, R., Chauhan, G., Traylor, M., Sargurupremraj, M., Okada, Y., Mishra, A., ... & Elliott, P. (2018). Multiancestry genome-wide association study of 520,000 subjects identifies 32 loci associated with stroke and stroke subtypes. Nature genetics, 50(4), 524-537.

Mestre, H., Kostrikov, S., Mehta, R. I., & Nedergaard, M. (2017). Perivascular spaces, glymphatic dysfunction, and small vessel disease. *Clinical science*, *131*(17), 2257-2274.

Narayan, S. K., Gorman, G., Kalaria, R. N., Ford, G. A., & Chinnery, P. F. (2012). The minimum prevalence of CADASIL in northeast England. Neurology, 78(13), 1025-1027.

Nation, D. A., Sweeney, M. D., Montagne, A., Sagare, A. P., D'Orazio, L. M., Pachicano, M., ... & Zlokovic, B. V. (2019). Blood–brain barrier breakdown is an early biomarker of human cognitive dysfunction. Nature medicine, 25(2), 270-276.

Nation, D. A., Sweeney, M. D., Montagne, A., Sagare, A. P., D'Orazio, L. M., Pachicano, M., ... & Zlokovic, B. V. (2019). Blood–brain barrier breakdown is an early biomarker of human cognitive dysfunction. Nature medicine, 25(2), 270-276.

Østergaard, L., Engedal, T. S., Moreton, F., Hansen, M. B., Wardlaw, J. M., Dalkara, T., ... & Muir, K. W. (2016). Cerebral small vessel disease: capillary pathways to stroke and cognitive decline. Journal of Cerebral Blood Flow & Metabolism, 36(2), 302-325.

Pantoni, L. (2010). Cerebral small vessel disease: from pathogenesis and clinical characteristics to therapeutic challenges. The Lancet Neurology, 9(7), 689-701.

Pasi, M., & Cordonnier, C. (2020). Clinical relevance of cerebral small vessel diseases. Stroke, 51(1), 47-53.

Peng, W., Achariyar, T. M., Li, B., Liao, Y., Mestre, H., Hitomi, E., ... & Deane, R. (2016). Suppression of glymphatic fluid transport in a mouse model of Alzheimer's disease. Neurobiology of disease, 93, 215-225.

Petersen, M. A., Ryu, J. K., & Akassoglou, K. (2018). Fibrinogen in neurological diseases: mechanisms, imaging and therapeutics. Nature Reviews Neuroscience, 19(5), 283-301.

Poels, M. M., Vernooij, M. W., Ikram, M. A., Hofman, A., Krestin, G. P., van der Lugt, A., & Breteler, M. M. (2010). Prevalence and risk factors of cerebral microbleeds: an update of the Rotterdam scan study. Stroke, 41(10_suppl_1), S103-S106.

Prince, M., Wimo, A., Guerchet, M., Ali, G. C., Wu, Y. T., & Prina, M. (2015). World Alzheimer Report 2015. The Global Impact of Dementia: An analysis of prevalence, incidence, cost and trends (Doctoral dissertation, Alzheimer's Disease International).

Prins, N. D., van Dijk, E. J., den Heijer, T., Vermeer, S. E., Koudstaal, P. J., Oudkerk, M., ... & Breteler, M. M. (2004). Cerebral white matter lesions and the risk of dementia. *Archives of neurology*, *61*(10), 1531-1534.

Rajani, R. M., Quick, S., Ruigrok, S. R., Graham, D., Harris, S. E., Verhaaren, B. F., ... & Williams, A. (2018). Reversal of endothelial dysfunction reduces white matter vulnerability in cerebral small vessel disease in rats. Science translational medicine, 10(448), eaam9507.

Rasmussen, M. K., Mestre, H., & Nedergaard, M. (2018). The glymphatic pathway in neurological disorders. The Lancet Neurology, 17(11), 1016-1024.

Rost, N. S., Cougo, P., Lorenzano, S., Li, H., Cloonan, L., Bouts, M. J., ... & Wu, O. (2018). Diffuse microvascular dysfunction and loss of white matter integrity predict poor outcomes in patients with acute ischemic stroke. Journal of Cerebral Blood Flow & Metabolism, 38(1), 75-86.

Schain, A. J., Melo-Carrillo, A., Strassman, A. M., & Burstein, R. (2017). Cortical spreading depression closes paravascular space and impairs glymphatic flow: implications for migraine headache. Journal of Neuroscience, 37(11), 2904-2915.

Serlin, Y., Shelef, I., Knyazer, B., & Friedman, A. (2015, February). Anatomy and physiology of the blood–brain barrier. In Seminars in cell & developmental biology (Vol. 38, pp. 2-6). Academic Press.

Singh, A., Bonnell, G., De Prey, J., Buchwald, N., Eskander, K., Kincaid, K. J., & Wilson, C. A. (2023). Small-vessel disease in the brain. American Heart Journal Plus: Cardiology Research and Practice, 27, 100277.

Thrane, V. R., Thrane, A. S., Plog, B. A., Thiyagarajan, M., Iliff, J. J., Deane, R., ... & Nedergaard, M. (2013). Paravascular microcirculation facilitates rapid lipid transport and astrocyte signaling in the brain. Scientific reports, 3(1), 2582.

Wang, M., Ding, F., Deng, S., Guo, X., Wang, W., Iliff, J. J., & Nedergaard, M. (2017). Focal solute trapping and global glymphatic pathway impairment in a murine model of multiple microinfarcts. Journal of Neuroscience, 37(11), 2870-2877.

Wardlaw, J. M., Doubal, F. N., Valdes-Hernandez, M., Wang, X., Chappell, F. M., Shuler, K., ... & Dennis, M. S. (2013). Blood–brain barrier permeability and long-term clinical and imaging outcomes in cerebral small vessel disease. Stroke, 44(2), 525-527.

Wardlaw, J. M., Makin, S. J., Hernández, M. C. V., Armitage, P. A., Heye, A. K., Chappell, F. M., ... & Thrippleton, M. J. (2017). Blood-brain barrier failure as a core mechanism in cerebral small vessel disease and dementia: evidence from a cohort study. Alzheimer's & Dementia, 13(6), 634-643.

Wardlaw, J. M., Smith, C., & Dichgans, M. (2019). Small vessel disease: mechanisms and clinical implications. The Lancet Neurology, 18(7), 684-696.

Wardlaw, J. M., Smith, E. E., Biessels, G. J., Cordonnier, C., Fazekas, F., Frayne, R., ... & Dichgans, M. (2013). Neuroimaging standards for research into small vessel disease and its contribution to ageing and neurodegeneration. The Lancet Neurology, 12(8), 822-838.

Wei, H., Jiang, H., Zhou, Y., Xiao, X., Zhou, C., & Ji, X. (2023). Vascular endothelial cells: a fundamental approach for brain waste clearance. Brain, 146(4), 1299-1315.

Zhang, C. E., Wong, S. M., Uiterwijk, R., Backes, W. H., Jansen, J. F., Jeukens, C. R., ... & Staals, J. (2019). Blood–brain barrier leakage in relation to white matter hyperintensity volume and cognition in small vessel disease and normal aging. Brain imaging and behavior, 13, 389-395.